Photoluminescence Properties of Multinuclear Copper(I) Compounds

Peter C. Ford,*,† Elena Cariati,†,‡ and James Bourassa†

Department of Chemistry, University of California, Santa Barbara, California 93106-9510, and Centro C.N.R., CSSSCMTBSO, Universitá di Milano, via Venezian 21, 20133 Milano, Italia

Received April 12, 1999 (Revised Manuscript Received September 21, 1999)

Contents

I. Introduction

The goal of this review is to outline the rich photophysical behavior of a remarkable series of luminescent polynuclear complexes of copper(I). Cuprous clusters display a wide variety of structural formats that are characterized by strikingly different emissive behavior. Systems ranging from the mononuclear CuI(3-Mepy)$_3$ to the stair-step polymer [CuIpy]$_\infty$ have been prepared from the simple combination of cuprous iodide and pyridine-based ligands in differing ratios. Since the d^{10} electronic configuration of Cu(I) enforces no stereochemical demands, the coordination sphere (normally four coordinate) is therefore largely determined by electrostatic and molecular mechanical factors. Furthermore, Cu(I) complexes in solution are quite labile to ligand substitution; thus, the species present are defined by thermodynamic stabilities rather than by kinetic control. For example, solutions of {CuIpy}$_n$ are primarily present as the tetrahedral clusters, Cu_4I_4-py$_4$, unless forced by the mass action law under high pyridine concentrations to mononuclear or dinuclear structures. On the other hand, crystalline solids isolated from such solutions may be in either tetranuclear or polymeric forms, depending on the crystallization conditions, especially solvent. As will be seen below, the structural ambiguities of these systems provide an additional challenge to the photophysical characterization of these materials.

The structural diversity of these systems can be illustrated by examining the cuprous halide complexes with ligands such as an aliphatic or aromatic nitrogen heterocycles. Crystallographic studies have demonstrated that complexes of Cu(I), I^-, and a particular ligand L form in a variety of structures depending on the stoichiometry (Figure 1). For a 1:1:1 Cu(I):I:L ratio, the most commonly encountered motif is the tetranuclear "cubane" structure ($Cu_4I_4L_4$) in which a tetrahedron of copper atoms is included by a larger I_4 tetrahedron with each I on a triangular face of the Cu_4 tetrahedron and the fourth coordination site of each copper is occupied by the ligand (L).[1] For stoichiometry 1:1:2, the most common structure displayed is an isolated rhombohedron of Cu_2I_2 with alternating copper and halide atoms (for example, [CuI(3-picoline)$_2$]$_2$).[2] Compounds of stoichiometry 1:1:3 have also been reported, for example, CuI(3-picoline)$_3$ which exists as a mononuclear complex with the Cu and I lying on a 3-fold axis.[3] In some cases, CuI−N donor ligand complexes of the same stoichiometry (1:1:1) exist in more than one crystalline format. For example, $Cu_4I_4py_4$ has a cubane form whereas {CuIpy}$_\infty$ is a polymeric "stair" formed by an infinite chain of steps.[4]

Luminescence in first-row transition metal complexes is frequently bypassed by the presence of low-lying ligand-field excited states (ES) which may be too short-lived to have measurable emissions.[5] In this context, filled-shell d^{10} systems offer an opportunity to observe other excited states. Several earlier reviews[6] have addressed the photophysical properties of mononuclear copper(I) complexes; here we will concentrate on the emission behavior of polynuclear copper (I) compounds. It should also be noted that other d^{10} coinage metal complexes often demonstrate similar behavior (see below).

In various tables below are collected data regarding the emission maxima and lifetimes of an extensive list of multinuclear cuprous luminophors. Such lists illustrate the range of systems that have been

* To whom correspondence should be addressed.
† University of California, Santa Barbara.
‡ Universitá di Milano.

10.1021/cr960109i CCC: $35.00
Published on Web 11/06/1999

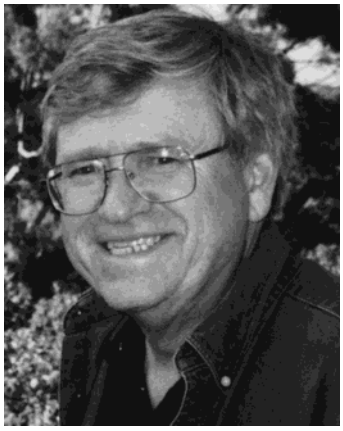

Peter C. Ford was born in California in 1941. His undergraduate work at Caltech (B.S. with Honors, 1962) was followed by graduate study with Kenneth Wiberg at Yale University (Ph.D., 1966) and an NSF Postdoctoral Fellowship with Henry Taube at Stanford University. In 1967 he joined the faculty of the University of California, Santa Barbara, where he has held the rank of Professor since 1977 and served as Department Chair for the period 1994–6. He has supervised the research of more than 40 students who have completed Ph.D. theses as well as for numerous B.S. and M.S. students and postdoctoral fellows. His current research interests include the mechanisms of catalytic activation of CO and other small molecules, the photochemistry and photophysics of coordination and organometallic compounds, and the bioinorganic applications of metal complex photoreactions.

Elena Cariati was born in Tradate, Italy, in 1968. She completed her Ph.D. degree in 1995 at the University of Milano. Her doctoral research, performed under the supervision of Professor Renato Ugo, was concerned with the use of silica as a reaction medium for the high-yield synthesis of various metal carbonyl compounds. In 1997 she spent one year as a Fullbright Fellow with Professor Peter C. Ford's group at the University of California, Santa Barbara. During this year she studied the nonlinear optical and luminescence properties of different Cu(I) complexes. In 1998 she joined the C.N.R. Research Center located at the University of Milano as Researcher. Her current research interests include study of the quadratic hyperpolarizability enhancement of organic molecules upon coordination to organometallic moieties.

investigated but do not really touch upon the extraordinarily rich photophysical behavior individual polynuclear complexes exhibit. We illustrate this briefly with the luminescence spectrum of the Cu_4I_4-py_4 cluster (**A**) which will be discussed further. In ambient temperature solution, **A** displays two distinct emission bands which also demonstrate different emission lifetimes.[7,8] The strong lower energy (LE) emission was assigned to a triplet cluster-centered (^{3}CC) ES, a combination of iodide to copper charge transfer (XMCT) and d−s transitions, and the weaker higher energy (HE) band to a triplet halide

James L. Bourassa was born in Maine in 1970. He received his B.S. degree in Chemistry from the University of Maine in 1992, where he worked with Professor Howard Patterson on inorganic photoluminescence. He earned his Ph.D. degree at the University of California, Santa Barbara (1998), under Professor Peter C. Ford. His doctoral research included photophysical studies of a diverse number of inorganic complexes, focusing upon the photochemical delivery of nitric oxide to biological targets and the photoluminescent properties of multinuclear cuprous compounds. He began postdoctoral work in the laboratory of Professor John T. Groves at Princeton University in 1999, and his current research interests include kinetic studies of ferric porphyrin complexes.

to ligand charge transfer (^{3}XLCT) ES.[7,8] These photophysical properties demonstrate marked environmental sensitivity, i.e., the spectra change reversibly by varying the temperature or rigidity of the medium. Accordingly, in frozen 77 K solution, the HE band is much more prominent and the LE emission maximum (λ_{max}^{em}) is shifted sharply to shorter wavelength. Such spectral shifts are even more prominent for other complexes such as the 4-phenylpyridine analogue (Figure 2). Thus, lowering the temperature leads to dramatic changes in the luminescence color the eye detects, a phenomenon described by Hardt as "luminescence thermochromism".[9] While not all coinage metal clusters display this breadth of environmental sensitivity, such diversions have generated considerable curiosity driven research.

II. Tetranuclear Cuprous Halide Clusters

It was noted above that the structure most commonly found for 1:1:1 mixtures of Cu(I), X^-, and a monodentate ligand L is tetranuclear with the Cu_4X_4 cluster core appearing as a distorted cubane as shown in Figure 1. The distances between the four tetrahedrally oriented copper centers are functions of both the halide X and the ligand L. For example, respective tetranuclear complexes of the types $Cu_4Cl_4L_4$ and $Cu_4I_4L_4$ demonstrate cubane configurations, but in the case of cuprous chloride cubanes, the Cu−Cu distance d_{CuCu} tends to be considerably longer[10] than in **A**, where d_{CuCu} (2.69 Å)[1] is less than the sum of the van der Waals radii (2.8 Å). Indeed, the $\{CuI\}_4$ core of the former might be described better as a Cu_4 tetrahedron included within a larger I_4 tetrahedron as illustrated by the space-filling model shown in Figure 3. Notably, the iodide complex is strongly luminescent at ambient temperature as a solid and moderately so in solution, while the chloride derivative shows no luminescence in fluid solution and only weak room temperature emission as a solid.[11] (The

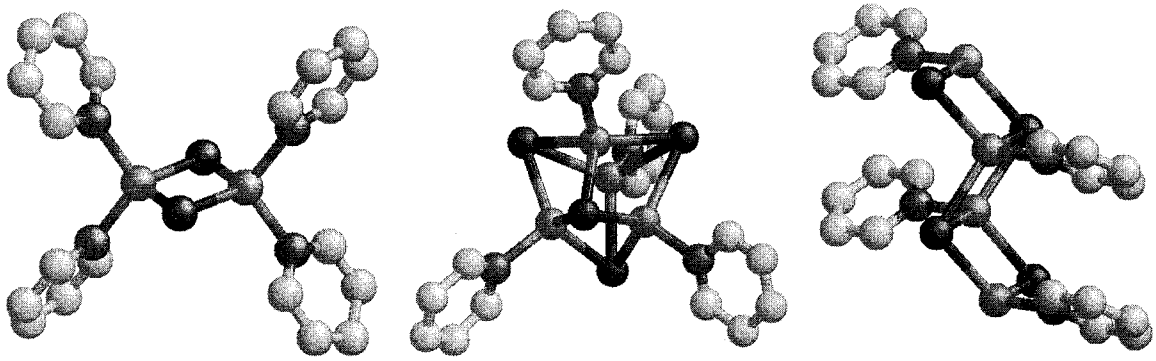

Figure 1. Illustrations of $Cu_2I_2py_4$, $Cu_4I_4py_4$, and the repeating unit of a "stairstep" polymer $\{CuIpy\}_n$ oligomers redrawn from the structural data.

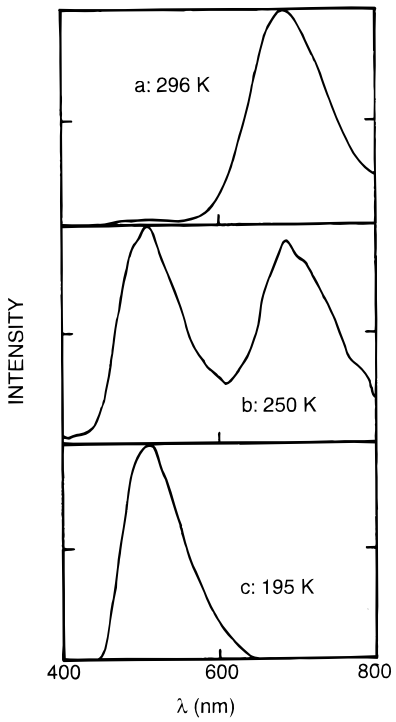

Figure 2. Temperature dependence of the emission spectrum of Cu_4I_4(4-phenylpyridine)$_4$ in toluene solution with relative intensities normalized to 1 in each case. (Reprinted with permission from ref 7. Copyright 1991 American Chemical Society.)

solids of both are quite luminescent at 77 K.) Also, the cuprous iodide clusters tend to be more stable than the chloro or bromo analogues. For these reasons, members of the Cu_4I_4(py-x)$_4$ series (where py-x is a substituted pyridine) have been the subjects of the majority of quantitative photophysical studies concerned with cuprous halide clusters. Table 1 summarizes some photoemission properties of various $Cu_4X_4L_4$ clusters.[2,4,7,12−21]

A. Cu_4I_4 Clusters

Interest in the luminescence properties of such clusters goes back to the pioneering studies by Hardt and co-workers[9,22,23] who noted the presence of at least three different complexes of the formula $CuIL_n$ (n = 1, 2, or 3), all of which are luminescent. They also discovered that the emission spectra of {CuI(py-x)} solids are markedly temperature dependent and

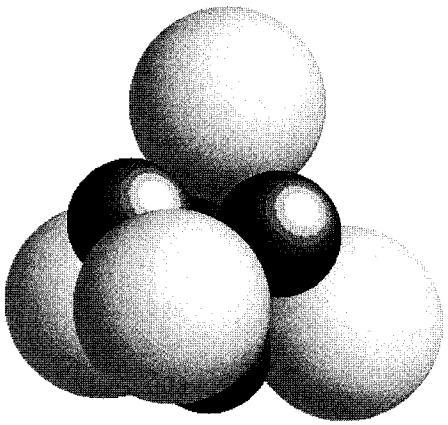

Figure 3. Space filling model of Cu_4I_4 core of $Cu_4I_4py_4$. Coordinates taken from the crystal structure data.

coined the term "luminescent thermochromism". As was discussed in the Introduction, the marked temperature dependence of the apparent color of the luminescence from the solids results in part from modest temperature-respondent shifts in λ_{max}^{em} but the more important contributions are the changes in the relative intensities of the higher energy (HE) and lower energy (LE) emission bands (Figure 4).[7,8] The relative intensities vary sharply with temperature; the LE band dominates at room temperature, while the HE band is quite prominent at temperatures below 80 K. However, as is illustrated in Figure 4, this effect is also dependent on the excitation source, especially at low T. It is also further notable that solid $Cu_4I_4py_4$ is white, and its dilute solutions are colorless with no significant absorptions in their optical spectra above 400 nm, yet in solution it emits deep into the red. UV absorptions increase toward shorter wavelengths with strong bands below 300 nm due to the presence of iodide and pyridine. Diffuse reflectance spectra of the solid display weak transitions in the 300−400 nm region.[7]

The thermochromic luminescence from solid $Cu_4I_4py_4$ was subsequently examined more quantitatively by Radjaipour and Oelkrug.[24] They also reported that the LE and HE emission bands demonstrated different excitation spectra and lifetimes, and this has been since confirmed by Kyle et al.[7] At 15 K, the HE emission displayed a longer lifetime (τ_{em} = 35 μs) but a lower energy excitation maximum (λ_{ex} = 370 nm) than that found for the LE emission (24 μs and 328 nm, respectively). Thus, the Stokes shift (which we

Table 1. Luminescent Properties of Tetranuclear Copper(I) Halide Clusters

compound	medium	λ_{max}^{em} (nm)	λ_{max}^{ex} (nm)	τ_{em} (μs)	ref
$[Cu_4I_4py_4]$	solid, 298 K	580	380	11.1	7
	solid, 77 K	438, 619	365, 330	23.2, 25.5	7
	Me methacrylate resin	610			12
	toluene, 298 K	480, 690	352, 325	0.45, 10.6	7
	toluene, 77 K	436, 583	350, 317	32.9, 26.5	7
	Me_2CO, 298 K	690		3.7	13
	CH_2Cl_2, 298 K	694		3.2	13
$[Cu_4I_4(py\text{-}d_5)_4]$	solid, 298 K	580			7
	solid, 77 K	433, 619			
$[Cu_4Cl_4py_4]$	solid, 298 K	527	425	4.0	11
	solid, 77 K	519	403	11.4	
	toluene, 77 K	577		21.4	
$[Cu_4I_4(4\text{-}^t\text{-Butylpy})_4]$	solid, 298 K	623			7
	solid, 77 K	437, 650	362, 327	29.2, 38.8	7
	toluene, 298 K	468, 696		0.35, 10.3	7
	toluene, 77 K	434, 595		38.7, 43.5	7
	Me_2CO, 298 K	690	362	5.3	13
	CH_2Cl_2, 298 K	712	327	5.2	13
	benzene, 298 K	473, 698		0.40, 11.1	14
$[Cu_4I_4(4\text{-benzylpy})_4]$	toluene, 298 K	473, 692		0.56, 11.0	7
	benzene, 298 K	486, 693		0.56, 11.6	14
$[Cu_4I_4(4\text{-phenylpy})_4]$	toluene, 298 K	520, 694		0.12, 9.4	7
	toluene, 77 K	505			7
	CH_2Cl_2, 298 K	701		3.7	13
	benzene, 298 K	520, 694		0.13, 10.2	14
$[Cu_4Cl_4(4\text{-phenylpy})_4]$	solid, 298 K	620	357, 459	0.87	11
	solid, 77 K	613	360,448	3.8	
	toluene, 77 K	584		18.7	
	CH_2Cl_2, 77 K	596		4.6	
$[Cu_4I_4(3\text{-chloropy})_4]$	toluene, 298 K	537, 675		0.35, 12.7	7
$[Cu_4I_4(3\text{-picoline})_4]$	solid, 298 K	588	382	11.1	2
	solid, 15 K	457, 588	373, 333	26.7	
$[Cu_4I_4(quin)_4]$	solid, 235 K	625			15
	solid, 15 K	490, 500, 526, 535, 565, 610			
$[Cu_4I_4(P(nBu)_3)_4]$	toluene, 298 K	654		2.23	14
$[Cu_4Cl_4(DEN)_4]$	solid, 77 K	530	357, 400	28.2	11
	toluene, 77 K	600	438	13.6	
	CH_2Cl_2, 77 K	560		9.0	
$[Cu_4I_4(morph)_4]$	solid, 298 K	625	355, 377, 392		16
	solid, 77 K	660	355, 375		16
	benzene, RT	654		0.3	12
	toluene, RT	671		0.51	7
	toluene, 77 K	630		19.8	7
$[Cu_4Cl_4(morph)_4]$	solid, 77 K	626			11
$[Cu_4I_4(pip)_4]$	solid, 298 K	590	413	12.3	4, 7
	solid, 77 K	590	357	13.4	
	toluene, 298 K	680	330	0.11	
	toluene, 77 K	638	318	19.8	
$[Cu_4I_4(dpmp)_4]$	solid, 298 K	440, 462 (sh), 570 (sh)	370	7.5	17
	solid, 77 K	446 (sh), 467	333 (sh), 360, 372 (sh)	18.1	
	MeCN, 77 K	500	339	15.3	
$[Cu_4Cl_4(dpmp)_4]$	solid, 298 K	500	360	2.7	17
	solid, 77 K	505	330 (sh), 366, 383 (sh)	10.0	
	MeCN, 77 K	530	341	12.8	
$[Cu_4Br_4(dpmp)_4]$	solid, 298 K	480, 626 (sh)	360	0.54	17
	solid, 77 K	487	327 (sh), 357, 374 (sh)	10.0	
	MeCN, 77 K	512	341	12.5	
$[Cu_4I_4(dmpp)_4]$	solid, 15 K	664		15, 58	18
$[Cu_4Cl_4(dmpp)_4]$	solid, 10 K	671			18
$[Cu_4Br_4(dmpp)_4]$	solid, 15 K	662			18
$[Cu_4I_4(MeCN)_4]\cdot$dibenzo-18-crown-6	solid, 298 K	550			19
	solid, 77 K	580			
$[Cu_4I_4(MeCN)_2(2,6\text{-dimethylaniline})]$	solid, 298 K	568			20
	solid, 10 K	560			
$[Cu_4I_4(MeCN)_2(o\text{-ethylaniline})_2]$	solid, 298 K	575			20
	solid, 10 K	575			
$[Cu_4I_4(MeCN)_2(6\text{-ethyl-}o\text{-toluidine})_2]$	solid, 298 K	568			20
	solid, 10 K	568			
$[Cu_4I_4(MeCN)_2(p\text{-anisidine})_2]$	solid, 298 K	608			20
	solid, 10 K	608			
$[Cu_4I_4(MeCN)_2(p\text{-toludine})_2]$	solid, 298 K	572			20, 21
	solid, 10 K	602			
$[Cu_4I_4(CH_3CN)_2(p\text{-chloroaniline})_2]$	solid, 298 K	630			20, 21
	solid, 10 K	628			

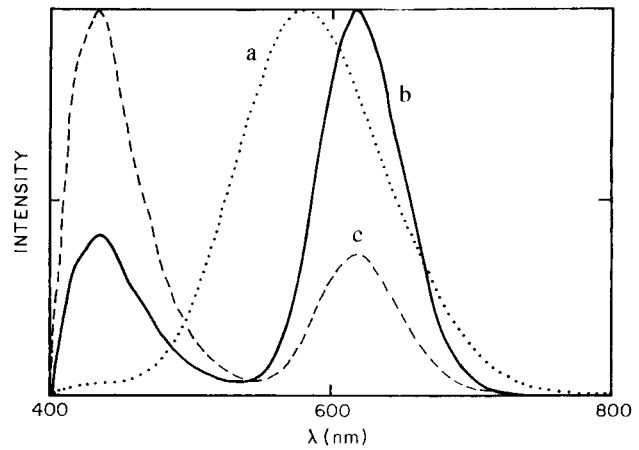

Figure 4. Normalized solid-state spectrum of $Cu_4I_4py_4$. (a) Spectrum at 295 K ($\lambda^{ex} = 380$ nm). (b) Spectrum at 77 K ($\lambda^{ex} = 330$ nm). (c) Spectrum at 77 K ($\lambda^{ex} = 365$ nm). (Reprinted with permission from ref 7. Copyright 1991 American Chemical Society.)

will define here as simply the energy difference between the excitation and emission maxima, $\nu_{max}^{ex} - \nu_{max}^{em}$) is much greater for the LE emission. The relatively long lifetimes in low-temperature solids as well as for solutions (see below) suggest that both emissions are spin forbidden; hence, the relevant excited states have triplet spin multiplicity. At 15 K, the HE emission band displayed some vibronic structure characteristic of the ligand, and Radjaipour and Oelkrug proposed that this band represents emission from a pyridine-centered $\pi\pi^*$ state.[24] They did not make a definitive proposal regarding assignment of the LE band, although a metal to ligand (i.e., pyridine) charge transfer (MLCT) excited state of $d^9\pi_L^*$ orbital parentage had previously been proposed by Hardt to explain this emission.[16] Radjaipour and Oelkrug also examined the ratio of intensities of the two bands over a range of temperatures, and based on a simple model of two emitting states, they calculated an activation energy of 9.9 kJ/mol for the internal conversion from the HE state to the LE state.

The question of assigning the LE band was again addressed in a 1986 report by Vogler and Kunkely,[12] who noted that the ambient temperature, solution-phase emission spectrum of the saturated amine cluster Cu_4I_4(morpholine)$_4$ ($\lambda_{max} = 654$ nm in benzene) mimics the broad red emission from $Cu_4I_4py_4$ (698 nm) under comparable conditions. Both appeared to show only the LE band, and although emission from the morpholine complex was considerably less intense, the band positions and shapes were similar. Thus, π-unsaturated ligand orbitals cannot be involved in the LE transition, so the MLCT excited state assignment proposed earlier is excluded. Instead, Vogler proposed that a metal-centered (MC) excited state of d^9s^1 orbital parentage, modified by Cu−Cu interactions within the Cu_4 cluster, was responsible for the emission. The large Stokes shift was attributed to the distortions between ES and GS structures owing to this excited state internuclear interaction. For comparison purposes, it might be noted that emission spectra of mononuclear Cu(I) centers doped into various inorganic glasses have been reported to display λ_{max} in the 430−500 nm range.[6d] These bands have been attributed to MC excited states, although some mixing with other configurations has been suggested.[6d] The question of excited state assignments of the clusters will be discussed at greater length below.

Table 2. Comparison of Cu−Cu Distances to Emissive Properties for Different Cuprous Iodide Complexes[20]

complex	Cu−Cu distance, d_{CuCu} (Å)	λ_{max}^{em}, HE (nm)	λ_{max}^{em}, LE (nm)
$Cu_4I_4py_4$	2.69	436	615
$Cu_4I_4(3-pic)_4$	2.65−2.75	457	588
$Cu_4I_4morph_4$	2.65		625
$Cu_4I_4pip_4$	2.66		570
$Cu_4I_4(CH_3CN)_4 \cdot Bz_2-18C_6$	2.77		550
$Cu_4I_4(CH_3CN)_2(p\text{-tld})_2$	2.70	458	586
$[Cu_2I_2(CH_3CN)(p\text{-ClAn})]_2$	2.68	420	628
$[CuIpy]_\infty$	2.88	449	

Correlations between structure and photophysical properties have been the subject of continuing attention for the tetranuclear copper(I) halide complexes with N-donor cyclic aromatic and aliphatic amines. In an early study of various solid $Cu_4I_4L_4$ (L = py, Et-py, pip, morph), Hardt and Pierre suggested a relationship between the thermochromic behavior of the LE band and the crystal symmetry.[16] Specifically they observed that more symmetrical systems, e.g., those with the $\bar{4}$ internal symmetry element displayed, a smaller red shift upon lowering T. Holt and co-workers investigated the possible parallel of symmetry and thermochromism further by preparing mixed-ligand clusters of the type $Cu_4I_4L_2L'_2$, thus eliminating the $\bar{4}$ element.[20,21] For the spectra of solid $Cu_4I_4(p\text{-tld})_2(CH_3CN)_2$ and $Cu_4I_4(p\text{-ClAn})_2(CH_3CN)_2$ (p-tld = p-toluidine and p-ClAn = p-chloroaniline), these authors observed in each case only small temperature-dependent shifts of the LE band. Thus, the absence of that symmetry element is not a central nor sufficient condition for such thermochromic behavior. These workers also substantiated the observation that the $Cu_4I_4L_4$and $Cu_4I_4L'_2(CH_3CN)_2$ solids showing a LE emission band ($\lambda_{max}^{em} = 570-630$ nm) have structures characterized by relatively short Cu−Cu distances ($d_{CuCu} < 2.8$ Å, Table 2).[20] Those with longer d_{CuCu} displayed little luminescence. The conclusion drawn from these observations was that d_{CuCu} rather than crystal symmetry is the crucial parameter defining the emission behavior. Only complexes with d_{CuCu} less than twice the van der Waals radius (1.4 Å) of Cu(I) showed the LE emission. These data reinforce the view that the longer wavelength luminescence derives from an ES involving more than one metal center.

Vogler's report[12] that the photophysical properties of $Cu_4I_4py_4$ in benzene solution follow behavior consistent with that expected for molecular species stimulated considerable further investigation by other research groups into the photophysical properties of these and other cuprous clusters. Notably, the observed emission from $Cu_4I_4py_4$ in benzene is deep red ($\lambda_{em} = 690$ nm), in contrast to the bright yellow emission of the solid ($\lambda_{em} = 580$ nm). This remarkable shift had been noted previously by Hardt, who proposed that the cubane cluster decomposed in

Table 3. Emission Spectral Data for Various $Cu_4I_4(py\text{-}x)_4$ in 294 K Toluene Solution[7]

	HE band[a,b]		LE band[a,b]	
L	λ_{max}^{em} ($\Delta\nu_{1/2}$)	E^{00}	λ_{max}^{em} ($\Delta\nu_{1/2}$)	E^{00}
4-*tert*-butylpyridine	468 (3.8)	26.3	696 (2.4)	17.5
4-benzylpyridine	473 (3.9)[c]	26.2	692 (2.4)	17.5
pyridine	480 (2.8)	24.5	690 (2.3)	17.5
4-phenylpyridine	520 (3.1)	23.2	694 (2.3)	17.4
3-chlorophyridine	537 (2.3)[c]	21.6	675 (2.5)	18.0

[a] λ_{max} in nm; $\Delta\nu_{1/2}$ in 10^3 cm^{-1}. [b] E^{00} in kK, estimated according to the "1% rule", namely, that E^{00} is estimated as the frequency where the band intensity is 1% that at λ_{max} on the high-energy side of the band. [c] From time-resolved spectra.

solution to dispersed cuprous iodide.[9] To refute this, Vogler et al. used osmometry to demonstrate that the $Cu_4I_4py_4$ and the related $Cu_4I_4(morph)_4$ cluster remained intact in solution. Furthermore, they also found that the LE emission from $Cu_4I_4py_4$ shifted to 610 nm when dissolved in polymethacrylate resin, a medium more viscous than fluid benzene but less so than are the pure solid or frozen solutions. This rigidochromic behavior was attributed to the likely molecular distortions occurring upon formation of the d−s excited state.

Subsequently, detailed studies were carried out by Kyle et al. on the photophysical behavior of $Cu_4I_4py_4$ (**A**) and of the analogous substituted-pyridine derivatives $Cu_4I_4(py\text{-}x)_4$.[7,14] Upon careful reinvestigation of the emission spectrum of **A** in room temperature toluene solution, the strong red LE emission at 690 was found to be accompanied by a very weak high-energy emission (λ_{em} = 480 nm). The respective lifetimes (τ_{em}) of the exponential decays of these bands were determined to be 10.6 and 0.45 μs, respectively. Quantum yield determinations in room temperature toluene solution for a variety of $Cu_4I_4L_4$ complexes gave values around 0.1 for the red emission and $<1 \times 10^{-3}$ for the blue band, those for **A** being $\Phi_{LE} = 0.09$ and $\Phi_{HE} = 3.4 \times 10^{-4}$.

A study of various $Cu_4I_4L_4$ (L = py, py-x, pip, and morph) in ambient temperature solutions demonstrated that the position of the LE band showed only modest dependence upon the nature of L and little dependence on the pyridine substituents.[7] In addition, the solution spectra of the compounds of the $Cu_4I_4(py\text{-}x)_4$ series each displayed the HE emission band (Figure 2), but, as noted above for the solid-state spectra, the blue emission was not present in the solution spectra at any T for $Cu_4I_4L_4$ clusters, if L were a saturated amine. Furthermore, it was the HE band that proved to be sensitive to the nature of the ligand substituents. Electron-donating pyridine substituents shift the band to the blue; electron-withdrawing substituents shift it to the red (Table 3). Investigation of solventochromic effects for $Cu_4I_4py_4$ revealed the LE band to be insensitive, while stronger donor solvents shift the high-energy band to shorter wavelengths. On the basis of these observations, assignment of the LE band was suggested by Kyle et al.[14] to be derived from a triplet cluster-centered (^{3}CC) excited state of d−s character, similar to the assignment previously drawn by Vogler. The term "cluster-centered" was coined[7,14] to emphasize that the relevant ES involves electronic delocalization over the Cu_4 core, the presumed LUMO being combined s and p orbitals having σ-bonding (metal−metal) symmetry. In addition, the substituent and solvent effects on the HE emission were argued to indicate radiative decay from a copper to py-x MLCT excited state. However, it should be noted that there were indications from preliminary calculations[7,14c] that iodide orbitals were major contributors to the highest occupied molecular orbitals of **A** (see below).

Also similar to the solid-state behavior was the observation that as T was lowered, the blue emission from **A** and related py-x complexes in toluene and other solutions increased greatly in relative intensity (Figure 2). In the lower temperature fluid solutions, this band underwent a blue shift while the LE band was observed to undergo a red shift. At the glass transition, the HE band, which is hardly discernible in the room temperature spectrum, becomes quite prominent and the LE band shifts sharply to the blue. Both bands display monoexponential decays, each with a distinct lifetime as well as distinctively different excitation maxima. This behavior is consistent with that also seen for the analogous structurally well characterized crystalline compounds. So it was concluded that the photophysical properties in solution were indeed representative of the molecular properties of intact $Cu_4I_4(py\text{-}x)_4$ clusters.[7] Furthermore, it was concluded that the dual emissions indeed represent radiative decay from two, individual, largely uncoupled emission states of the same molecular species and that internal conversion between these is relatively slow.

The natures of the excited states apparently responsible for the photophysical properties of **A** were further probed by ab initio calculations at the restricted Hartree−Fock self-consistent field level. Calculations were carried out by Vitale et al.[25] for the hypothetical complex $Cu_4I_4(NH_3)_4$ and for $Cu_4I_4py_4$ using effective core potentials for the metal atoms. These indicated the highest occupied molecular orbitals (HOMO) of both clusters to be largely (>80%) composed of iodide 5p-orbitals with only small contributions from the metal d orbitals. Thus, the earlier assignment of the HE emission as being from a MLCT state appears to be naïve; a more correct assignment would be that this state is largely I → py-x, i.e., halide to ligand charge transfer (XLCT), in character. The same calculations confirm the view that the lowest unoccupied molecular orbital (LUMO) of **A** is principally copper 4s in character, although delocalized over the Cu_4 core. Thus, if the LE emission is occurring from a state related to HOMO → LUMO excitation, this would have I → Cu (or more correctly I_4 → Cu_4) halide to metal charge transfer (XMCT) character. The empirical requirement of a short d_{Cu-Cu} drawn by Holt can thus be rationalized as derived from the nature of the acceptor orbital in this state.[11,17] In the CC excited state, electron density has moved from copper d orbitals to copper s orbitals, which are Cu−Cu bonding. Thus the energy of this ES and the shape of its potential surface are strongly dependent on the extent of Cu−Cu interac-

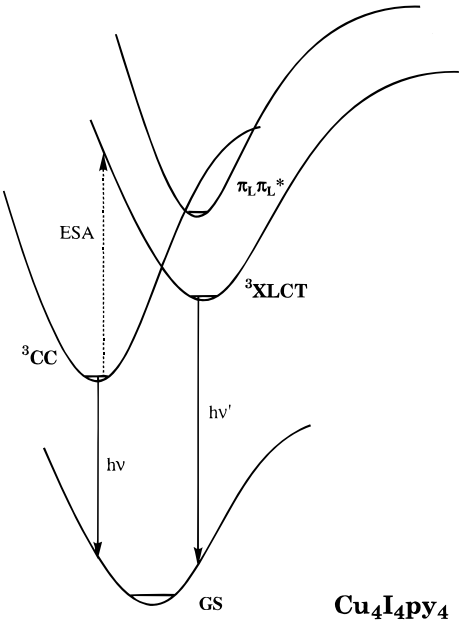

Figure 5. Proposed potential energy surface of $Cu_4I_4py_4$.

tion. A key point to emphasize here is that, despite the evolution of the excited state assignments, the experimental and early theoretical treatments consistently pointed to the HE emission as involving the π^* orbitals of ligands such as pyridine and the LE emission as involving Cu orbitals delocalized over the cluster.

Subsequently, more rigorous calculations by Vitale taking electronic reorganization into account led to the conclusion that the LE emission occurs from a state of mixed configuration delocalized over the Cu_4I_4 core with roughly equal contributions from d−s and XMCT components.[26] On the basis of these results, the large Stokes shift for the LE band was rationalized by the fact that {XMCT/d−s} excitation to give the CC excited state should lead to contraction of the Cu_4 core and to some expansion of the I_4 unit. The filled, highest energy d-orbitals are formally antibonding, while the empty s-orbitals are bonding with respect to the copper−copper interactions within the Cu_4 core. Hence, the structure of the ^{3}CC excited state should be significantly distorted from the GS configuration. On the other hand, XLCT excitation would leave the Cu−Cu and Cu−I interactions in the cluster core essentially undisturbed, in agreement with the much smaller Stokes shift related to this emission. Moreover, distortions of the ^{3}XLCT state would be along coordinates different from the distortion coordinates of a ^{3}{XMCT/d−s} cluster-centered ES. For this reason, it was proposed that these differences in the magnitude and direction of the respective distortion coordinates are responsible for the poor coupling between the two emissive states. Figure 5 represents a qualitative illustration of the types of states proposed to be responsible for the emission properties of $Cu_4I_4py_4$. The 0−0 energies (E^{00}) of the ^{3}XLCT and ^{3}CC states to which the HE and LE emission bands are attributed were estimated as 2.45 and 1.75 μm^{-1}, respectively, in toluene solution.[7]

B. Other Cu_4X_4 Clusters

The question one might now ask is what happens when the cluster is constructed from a different halide? Notable in this context are the photophysical studies reported by Ryu et al. for a series of cuprous chloride clusters $Cu_4Cl_4L_4$ (L = py, 4-Phpy, DEN, morph, and triethylamine) (DEN = diethylnicotinamide).[11] Two key observations were made. First, the py-x derivatives displayed a strong, relatively long-lived emission band in the solid state at 298 K that became much more intense at 77 K. However, no emission was seen at either *T* for the saturated amine ligands (L = morph or Et_3N). Second, for the py-x complexes, emission bands proved to be sensitive to the substituent, the energy falling in the order py ≥ DEN > 4-Ph-py. These data suggest that the Cu_4Cl_4(py-x)$_4$ emissions are most closely related to the HE emission bands of the iodide analogues, which theoretical studies suggest are XLCT in character.[25] Consistent with this conclusion is the observation that the ground state d_{CuCu} of the chloro complexes are longer than the ∼2.8 Å d_{CuCu} argued by Holt to be a necessary condition for the CC emission.

On the other hand, the Cu_4Cl_4(py-x)$_4$ complexes emit at significantly lower energies than the respective HE bands for their iodo analogues. This leads one to wonder how that observation matches with the assignment as XLCT emission given the known differences in the halide ion ionization potentials. Indeed, such reasoning was used to assign the luminescence of Cu_4Cl_4(DEN)$_4$ and related mixed-metal complexes as the result of a metal-localized ($d^9s^1 \rightarrow d^{10}$) transition.[27]

One problem in trying to compare spectra of Cu_4X_4-py_4 analogues is that changes in the halogen are usually accompanied by considerable structural differences as well. To address this issue, Ryu et al. extended photophysical studies to the homologous series Cu_4X_4(dpmp)$_4$ (X = Cl, Br or I; dpmp = 2-(diphenylmethyl)pyridine).[17] The advantage of this

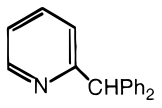

dpmp

series is that the variations in X are not accompanied by significant changes in the molecular or crystal structure.[28] Thus, the d_{CuCu} are nearly identical (≅2.90 Å) in the three isomorphous solids. At 77 K, both in the solid state and in glasses of acetonitrile solution, the luminescence spectrum of each Cu_4X_4-(dpmp)$_4$ derivative displayed a single band (e.g., Figure 6). The emission band energies from the three homologous complexes and the respective excitation spectra showed very few differences, although the emission energies did follow the order I > Br > Cl (Table 1). Notably, these bands were narrower, higher in energy, and displayed smaller Stokes shifts than the LE band of related Cu_4I_4(py-x)$_4$ compounds.[17]

The relative insensitivity of the 77 K emission and excitation spectra of the three Cu_4X_4(dpmp)$_4$ com-

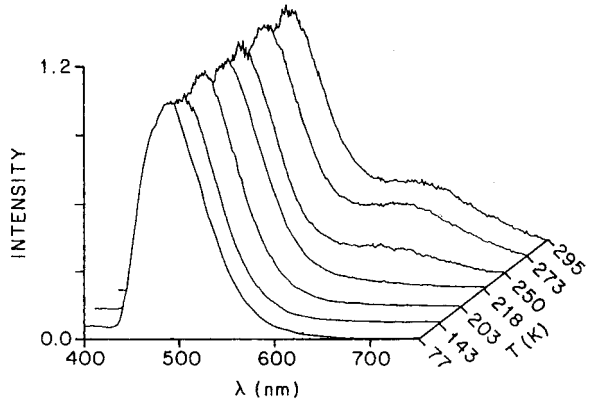

Figure 6. Temperature dependence of emission spectra of solid $Cu_4Br_4(dpmp)_4$, λ_{exc} = 380 nm. (Reprinted with permission from ref 17. Copyright 1993 American Chemical Society.)

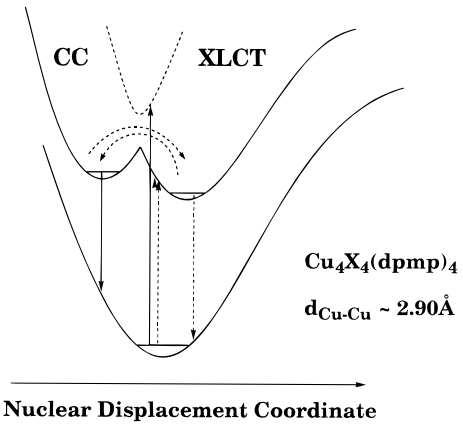

Figure 7. Proposed excited state surfaces for the 2-(diphenyl)methylpyrine complexes $Cu_4X_4(dpmp)_4$. (Reprinted with permission from ref 17. Copyright 1993 American Chemical Society.)

plexes to the identity of the halogen X might appear to argue against assignment of this emission to a XLCT excited state. The halide anion optical electronegativities and gas-phase ionization energies follow the order Cl > Br > I, and intuitively one might expect the ^{3}XLCT state energies to follow the same order. However, ab initio calculations demonstrate that the halide *ionicity* in the Cu_4X_4 clusters also follows the order Cl > Br > I, precisely because of the electronegativity differences.[17,26] As a consequence, coordinated iodide is less negatively charged than the analogous chloride, a feature which compensates for the lower ionization energy of the free I^- ion. Thus, 77 K emission bands of the respective $Cu_4X_4(dpmp)_4$ were assigned to ^{3}XLCT ES in analogy to the previous assignment for $Cu_4Cl_4py_4$. While the ab initio calculations are too imprecise to predict accurately the ^{3}XLCT excited state energies, they clearly rationalize the insensitivity of the XLCT energies to whether X is Cl, Br, or I. This result may have bearing with regard to the excited state properties of other metal halide complexes where assignments of charge transfer transitions involving coordinated halide were excluded owing to the relative independence of the emission energies to halide identity and the failure to consider the impact that changes in ionicity will have on the energies of XMCT or XLCT transitions.

While the 77 K solid-state spectra of the $Cu_4X_4(dpmp)_4$ complexes showed but a single XLCT band, at higher temperature, long wavelength shoulders were seen in the spectra of $Cu_4I_4(dpmp)_4$ and $Cu_4Br_4(dpmp)_4$ (e.g., Figure 6).[17] This feature was initially assigned to weak emission from a ^{3}CC excited state, although the lifetimes observed proved to be identical to the τ_{em} measured at the XLCT band maxima. This pattern, different from that for **A**, was attributed to thermal equilibrium between the ^{3}XLCT and ^{3}CC states. In these cases, the ^{3}CC state is apparently higher in energy by about 0.10 μm^{-1}, so the CC emission is observed only under conditions where there is some thermal population of this state, as illustrated by Figure 7. Comparison with Figure 4 illustrates the difference with ES surfaces suggested for $Cu_4I_4py_4$, where a barrier to internal conversion in **A** would result from the large distortion of the ^{3}CC state relative to the GS and ^{3}XLCT structures. Since the longer d_{CuCu} in the dpmp complexes diminishes metal orbital overlap, the ^{3}CC state in this case is no longer the lowest energy excited state. This leads to a lower barrier for internal conversion and to greater communication between the relevant ES.

C. Rigidochromic Effects

A general observation for the $Cu_4I_4L_4$ clusters is that the CC emission band shift occurs at a distinctly lower energy for fluid solutions than for the solid at the same temperature. Furthermore, when solutions cooled, the CC band first shifts to the red, then sharply to the blue at the glass transition. The XLCT band (when present) behaves differently. For example, the HE emission seen for $Cu_4I_4(4\text{-}^tBupy)_4$ solutions in toluene shows a gradual blue shift upon lowering T from 294 (468 nm) to 195 (450 nm) then to 77 K (434 nm), where the solution is frozen.[7] In contrast, the LE emission band shows a red shift from 696 nm at 294 K to 714 nm at 195 K, but a dramatic blue shift to 595 nm upon further cooling to 77 K. A related phenomenon was the observation by Vogler[12] that the emission from $Cu_4I_4py_4$ in polymethacrylate solutions lies at a λ_{max} between those of the solid and fluid solution at room T.

This behavior has been attributed to the effect of medium rigidity owing to distortion of the ^{3}CC state relative to the ground state. Similar behavior has been seen for the MLCT emission bands of rhenium(I) complexes such as $Re(phen)(CO)_3Br$ for which the term "rigidochromic effect" was coined.[29] An alternative way to probe this phenomenon is to perturb the solvent rigidity by variation of hydrostatic pressure P_{hyd} until the solvent freezes.[30] Such an experiment allows the study of luminescence rigidochromism in solution without changing T nor the identity of the solvent itself. Aromatic hydrocarbon solvents which can "freeze" at relatively low applied pressure P_f include benzene (P_f = 72 MPa at 298 K), *p*-xylene (36 Mpa), and *o*-xylene (229 MPa). For example, when a 298 K benzene solution of $Cu_4I_4py_4$ was subjected to hydrostatic pressure, the 695 nm CC emission disappeared when P_{hyd} was raised to 75

Table 4. Rate Constants and Activation Parameters for the Quenching of $[Cu_4I_4Py_4]$* by Various Quenchers in 296 K Dichloromethane Solution[31]

quencher[a]	$-E_{1/2}$[b] (V)	ΔG_{et}^{o} (V)[c]	10^{-7} k_q[d] (M^{-1} s^{-1})	$\Delta H^{\ddagger}$ (kJ mol^{-1})	$\Delta V^{\ddagger}$ [e] (cm^3 mol^{-1})
$Cr(acac)_3$	2.43	0.65	4.7	0.5 ± 0.9	-0.3 ± 0.2
$Cr(Bracac)_3$	1.89	0.11	6.9		
$Cr(dbm)_3$	1.87	0.09	4.6		
$Cr(3\text{-}SCNacac)_3$	1.66	−0.12	11.5		
$Cr(tfac)_3$	1.64	−0.14	10.9		
$Cr(3\text{-}NO_2acac)_3$	1.57	−0.21	7.6		
$Cr(tta)_3$	1.43	−0.35	8.1		
$Cr(tfbzac)_3$	1.43	−0.35	10.0	0.7 ± 0.2	$+0.2 \pm 0.2$
m-dinitrobenzene	1.37	−0.41	0.72	28 ± 1	-8.2 ± 0.4
o-dinitrobenzene	1.26	−0.52	0.42	40 ± 2	-7.0 ± 0.9
p-dinitrobenzene	1.18	−0.60	25.3		
1,4-benzoquinone	0.94	−0.84	129	5.4 ± 1.3	$+5.2 \pm 0.6$
$Cr(hfac)_3$	0.79	−0.99	141	1.1 ± 0.8	$+6.6 \pm 0.5$
$Me_{10}Fc^{+}$ [f]	0.49	−1.29	810		
Me_2Fc^{+}	0.15	−1.63	$\sim 1.2 \times 10^3$		
Fc^{+}	0.00	−1.78	1.2×10^3		$+6.2 \pm 0.5$

[a] Ligand abreviations: acac = 2,4-pentanedionate (acetylacetonate); dbm = 1,3-diphenyl-1,3-propanedionate; hfac = 1,1,1,5,5,5-hexafluoro-2,4-pentanedionate; Br-acac = 3-bromo-2,4-pentanedionate; SCNacac = 3-thiocyanato-2,4-pentanedionate; NO_2acac = 3-nitro-2,4-pentanedionate; tfac = 1,1,1-trifluoro-2,4-pentanedionate; tta = 4,4,4-trifluoro-1-(2-thienyl)-1,3-butanedionate; tfbzac = 4,4,4-trifluoro-1-phenyl-1,3-butanedionate. [b] Reduction potential vs ferrocenium/ferrocene in CH_2Cl_2.[14] [c] Free energy of the electron transfer reaction $\mathbf{I}^* + Q = \mathbf{I}^+ + Q^-$, calculated according to text using the value $E_{1/2}(\mathbf{I}^+/\mathbf{I}^*) = -1.78$ V; the estimated work term −0.14 V has not been added. [d] k_q from Stern−Volmer plots. [e] $\Delta V^{\ddagger}_i = -RT\,((\mathrm{d} \ln k_i)/(\mathrm{d}P))_T$. [f] Fc^+ = ferrocenium ion; $Me_{10}Fc^+$ = decamethylferrocenium ion, Me_2Fc^+ = dimethylferrocenium ion.

MPa accompanied by the concomitant growth of an emission at 575 nm. This transformation occurred sharply at the pressure corresponding to P_f and was fully reversed upon releasing the pressure. Perhaps surprisingly, τ_{em} underwent little change. Analogous results were obtained at the respective P_f values for *o*-xylene or *p*-xylene solutions. In each case, these did not involve a gradual shift in λ_{max}, but instead, one band quickly disappeared once $P_{hyd} > P_f$ while the other grew in. In contrast, there was little effect on the emission spectrum of **A** for P_{hyd} up to 350 MPa in toluene, which remains continuously fluid over this range. Thus, one can indeed conclude that the luminescence spectral shifts upon freezing at low *T* are largely the result of solution rigidity effects. Similar pressure experiments were carried out with the rhenium complex noted above, and it is notable that the CC band of **A** is considerably more sensitive to P_{hyd} induced phase transitions than is the MLCT band of $Re(phen)(CO)_3Br$.[30]

D. Excited State Energy and Electron Transfer

The long lifetimes characteristic of both the ^{3}XLCT and ^{3}CC excited states of the cuprous iodide clusters in solution lead one to consider the possibility of bimolecular processes. Among other information, the kinetics of such processes also provide further insight into the character of the excited state distortions. The quenching process can be visualized in terms of the excited cluster and quencher Q diffusing together to form a short-lived encounter complex (rate constant k_d) followed by diffusion apart (k_{-d}), energy transfer (k_{en}), or electron transfer (k_{el}) (eq 1). The measured

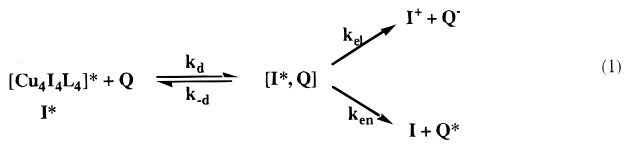

(1)

luminescent lifetime τ_m can be determined in the presence of various quencher concentrations [Q], and the rate constant for quenching can be determined from Stern−Volmer plots according to eq 2 in which τ_0 is the lifetime in the absence of quencher.

$$\tau_0/\tau_m = 1 + k_q\tau_0[Q] \qquad (2)$$

Qualitatively, the observation of emission from two, nearly uncoupled excited states of a $Cu_4I_4L_4$ cluster allows for the possibility of selective quenching of one or the other ES. This was realized in studies of emission from benzene solutions of **A**. Addition of biphenyl (triplet energy $E_T = 2.30$ μm^{-1}), naphthalene (2.13 μm^{-1}), or O_2 (0.78 μm^{-1}) to deaerated 294 K benzene solutions of **A** resulted in dynamic quenching of the HE emission.[7] For the first two, there was no effect on the LE emission lifetimes, but both emissions were quenched by O_2. Linear Stern−Volmer plots for biphenyl and naphthalene gave 3.5×10^8 and 6.6×10^9 M^{-1} s^{-1} as the respective k_q's for quenching of the HE state. For O_2, k_q values of $\geq 10^{10}$ M^{-1} s^{-1} for HE emission quenching and $k_q = 6.0 \times 10^8$ M^{-1} s^{-1} for LE emission quenching were estimated from a single [O_2] experiment. Notably, O_2 is the one acceptor among the three with an ES energy lower than that estimated for the ^{3}CC state (17.5 kK).

Energy and electron transfer quenching of the ^{3}CC emission of **A** by a series of different Q were also probed in detail for dichloromethane solutions, a medium in which the HE emission was too weak to observe. Both temperature and pressure effects on the k_q values were probed, and these are summarized in Table 4.[31] For a homologous series of tris(acetylacetonate) complexes of Cr(III), the k_q values vary from $\sim 5 \times 10^7$ to 1.4×10^9 M^{-1} s^{-1} at ambient temperature and pressure with the faster rates occurring with those CrL_3 complexes with the less negative reduction potentials. Each of these CrL_3 complexes has a low-lying ^2E_g state (1.2−1.3 μm^{-1}) which may participate in direct energy transfer quenching. This explains the moderate quenching of

A*, even by Cr(acac)$_3$ ($k_q \approx 5 \times 10^7$ M^{-1} s^{-1}) which has a very unfavorable one-electron reduction potential.

Quenchers with less negative reduction potentials demonstrate larger values of k_q (Table 4), so electron transfer from **A*** to Q must be considered as a quenching mechanism. The free energy for the excited state electron transfer quenching can calculated from

$$\Delta G_{el}^\circ = E_{1/2}(\mathbf{A}^+/\mathbf{A}^*) - E_{1/2}(\mathrm{Q}/\mathrm{Q}^-) \qquad (3)$$

where $E_{1/2}(\mathrm{Q}/\mathrm{Q}^-)$ is the reduction potential for the quencher and $E_{1/2}(\mathbf{A}^+/\mathbf{A}^*)$ is the potential for the hypothetical half-cell $\mathbf{A}^+ + e^- \rightarrow \mathbf{A}^*$. This can be estimated from

$$E_{1/2}(\mathbf{A}^+/\mathbf{A}^*) = E_{1/2}(\mathbf{A}^+/\mathbf{A}) - E^{00} \qquad (4)$$

where E^{00} is the ES energy and $E_{1/2}(\mathbf{A}^+/\mathbf{A})$ is the ground state reduction potential, ~0.28 V vs Fc$^+$/Fc (Fc = ferrocene). From the band maximum (691 ± 3 nm, 1.448 ± 0.006 μm^{-1}) and width (0.233 ± 0.004 μm^{-1}), both of which are remarkably solvent independent, the E^{00} value for the CC ES was estimated above as 1.75 μm^{-1} based on the 1% rule (see Table 3). However, Franck−Condon analyses of ligand-field emission bands in some Rh(III) complexes concluded that a 10% rule might be more appropriate.[32] If so, then E^{00} can be estimated as 1.66 μm^{-1} (2.06 V), which would give $E_{1/2}(\mathbf{A}^+/\mathbf{A}^*) = -1.78$ V. The data in Table 4 was analyzed using this more conservative value.[31]

According to steady-state analysis of the model illustrated in eq 1, k_q can be rewritten as

$$k_q = \frac{(k_{el} + k_{en})k_d}{k_{-d} + k_{en} + k_{el}} \qquad (5)$$

When $k_{-d} \gg (k_{el} + k_{en})$, this simplifies to $k_q = (k_d/k_{-d})(k_{el} + k_{en})$. At the other extreme, when $(k_{el} + k_{en}) \gg k_{-d}$, the reaction becomes diffusion-limited and $k_q = k_d$, the rate constant for bimolecular diffusion (~10^{10} M^{-1} s^{-1}). The latter situation was clearly demonstrated for the ferrocenium ions where ΔG_{el}° is large and negative.[31b] Furthermore, rates approaching the diffusion limit were also seen for benzoquinone ($k_q = 1.3 \times 10^9$ M^{-1} s^{-1}). For these quenchers, $\Delta H_q^\ddagger$ and $\Delta V_q^\ddagger$ values (Table 4) were consistent for a reaction approaching the diffusion rate limit, namely, modestly positive. This reflects the change in viscosity and corresponding slowing of diffusion as hydrostatic pressure is applied. In contrast, quenchers such as Cr(acac)$_3$ have very unfavorable values of ΔG_{el}°, so quenching must occur by energy transfer. The k_q values were smaller, and both $\Delta H_q^\ddagger$ and $\Delta V_q^\ddagger$ were found to be near zero. The more interesting cases are those quenchers for which electron transfer is less than diffusion-limited and is competitive with energy transfer. In these cases, substantially negative $\Delta V_q^\ddagger$ values were seen (Table 4), apparently reflecting the substantial outer-sphere solvent reorganization energy owing to charge separation accompanying the electron transfer **A*** + Q → $\mathbf{A}^+ + \mathrm{Q}^-$.[33] The same quenchers also demonstrated sizable activation enthalpies $\Delta H_q^\ddagger$.

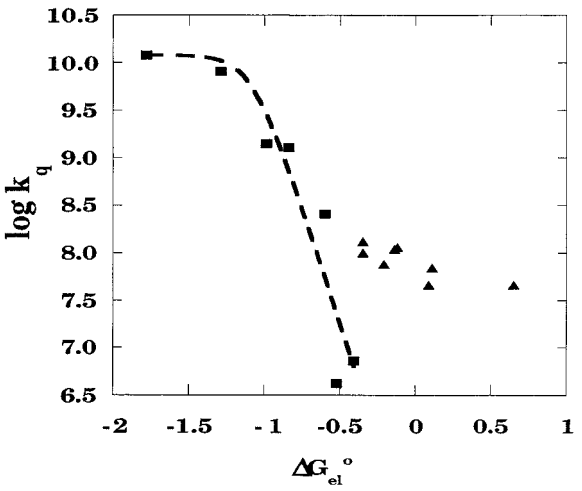

Figure 8. Fit of k_q values for the quenching of the cluster-centered excited state of $Cu_4I_4py_4$ by ferrocenium derivatives and various organic oxidants (squares) to the Marcus model for outer-sphere electron transfer (data from Table 4). The triangles represent Cr(III) tris(β-diketonate) complexes with low-lying ligand-field excited states which also quench by energy transfer. (Reprinted with permission from ref 316. Copyright 1994 American Chemical Society.)

According to electron transfer theory,[34] k_{el} should maximize when the driving force approaches the sum of the inner- and outer-sphere reorganization energies (i.e., when $-\Delta G_{el}^\circ = \lambda = \lambda_{is} + \lambda_{os}$). The data reported in Table 4 suggest that a driving force >1 V is required in order for k_q to approach k_d owing to a very large λ required by the **A***/$\mathbf{A}^+$ exchange. A major contribution to reorganization energy would be structural differences between **A*** and $\mathbf{A}^+$ given the major distortion of the ^{3}CC state from the corresponding ground state. This distortion is manifested in the large Stokes shift between excitation and emission maxima and in the ab initio calculations,[26] which conclude enhanced Cu−Cu bonding and decreased Cu−I bonding in the ES.

Figure 8 is a plot of $\log(k_q)$ as function of ΔG_{el}°. The curve shown represents the best least-squares fit of selected data from Table 4 (the k_q's for the ferrocenium derivatives, the nitroaromatics, and Cr(hfac)$_3$) to the equation

$$\frac{1}{k_q} = \frac{1}{k_d} + \frac{1}{K_a k_{el}'} \qquad (6)$$

The term K_a is the "equilibrium constant" (k_d/k_{-d}) for precursor complex formation (~1 M^{-1}) and k_{el}' is the rate constant for electron transfer in an outer-sphere precursor complex expressed as[33]

$$k_{el}' = \upsilon_n \kappa_e \exp\left[\frac{-(\Delta G_{el}^\circ + \lambda)^2}{4\lambda RT}\right] \qquad (7)$$

in which υ_n is the frequency factor and κ_e is the adiabaticity factor. The curve shown was obtained by allowing the product $K_a\nu_n\kappa_e$ and reorganization energy λ to iterate until an optimum fit ($R = 0.96$) was obtained. This gave a typical value of 1.5×10^{11} M^{-1} s^{-1} for $K_a\nu_n\kappa_e$ and a large value of 1.89 eV (183

Table 5. Emissive Properties of Other Cuprous Halide Polynuclear Complexes

compound	conditions	λ_{max}^{em} (nm)[a]	τ_{em} (μs)[c]	ref
$[Cu(py)_2]_2$	solid, 298 K	517		7
	solid, 77 K	510		
$[CuI(Et_4en)]_2$	solid, 298 K	522		7
	solid, 77 K	544		
$[CuI(quin)_2]_2$	solid, 251 K	620		15
	solid, 15 K	620		
$[CuI(PPh_3)py]_2$	solid, 298 K	444	11	36
	solid, 77 K	444	45	
$[CuCl(PPh_3)py]_2$	solid, 298 K	518	12−16	36
	solid, 77 K	521	22	
$[CuBr(PPh_3)py]_2$	solid, 298 K	487	16	36
	solid, 77 K	520	33	
$[Cu_3(DPMP)_2(MeCN)_2(\mu\text{-}Cl)_2][ClO_4]$	MeCN, 298 K	530	1.7	37
$[Cu_3(DPMP)_2(MeCN)_2(\mu\text{-}I)_2][ClO_4]$	MeCN, 298 K	560	3.1	37
$[CuIpy]_\infty$	solid, 298 K	437	7.6	4, 7
$[CuIMeCN]_\infty$	solid, 298 K	540		19
$[\{(Ph_3P)_2Cu_2(\mu\text{-}Cl)_2(\mu\text{-pyrazine})\}_\infty]$	solid, 20 K	612		39

kJ mol^{-1}) for λ.[31b] For comparison, a similar treatment of the redox quenching of the MLCT emission from the Cu(I) complex $Cu(dpp)_2^+$ (dpp = 2,9-diphenyl-1,10-phenanthroline) by several nitrobenzenes gives a reorganization energy of 0.62 eV.[35]

The outer-sphere contribution to the reorganization energy λ_{os} for electron transfer quenching of **A*** by Fc^+ can be estimated from the classical model to be about 0.5 eV.[31b] This leaves about 1.4 eV as the inner-sphere contribution λ_i. These large inner-sphere effects are apparently another consequence of the distortion of the ^{3}CC excited state cluster relative to the analogous ground state structures. As we will see below, similarly large reorganization energies are characteristic of excited state electron transfer quenching of other cuprous clusters.

E. Cu_4X_4(phosphines)$_4$

Although there has been considerably less photophysical investigation of tetranuclear $Cu_4X_4L_4$ clusters with L as a phosphine, the limited studies in this area suggest that these systems will also demonstrate similarly rich luminescence behavior. For example, the photoemission spectrum of $Cu_4I_4(P^nBu_3)_4$ in ambient temperature toluene solution displays a single broad band at 654 nm with a lifetime of 2.2 μs.[11] This behavior is reminiscent of that seen for the aliphatic amine complexes described above, and one is tempted to assign this to emission from the lowest energy cluster-centered {XMCT/d−s} ES.

Another phosphorus ligand which has been probed in this regard is pdmp (1-phenyl-3,4-dimethyl phosphole). Zink and co-workers have reported the low-

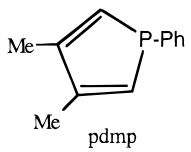

pdmp

temperature (15 K) luminescence from the homologous series $Cu_4X_4(pdmp)_4$.[18] The solids displayed λ_{max}^{em} at 671, 662, and 664 nm, respectively, for X = Cl, Br, and I. The vibronic structure of this band was quite evident for the iodo derivative, and the spectrum was analyzed by time-dependent theory of electronic spectroscopy in terms of seven vibrational modes also seen in the ground state Raman spectrum. On the basis of this result, the emission spectrum was assigned to a one-electron transition ending on the phosphole ligand. Between interpreting the transition as metal to pdmp ligand charge transfer (MLCT) or as a halide to phosphine ligand to ligand charge transfer (XLCT), the former was favored due to the lack of shift when going from $Cu_4Cl_4(pdmp)_4$ to $Cu_4Br_4(pdmp)_4$ and $Cu_4I_4(pdmp)_4$. However, it is notable that this series displays photophysical properties quite similar to those reported by Ryu et al.[17] for the $Cu_4X_4(pdmp)_4$ clusters. The latter article concluded from ab initio calculations that changes in halide ionicity dampen the differences in the halides in the XLCT transitions and lead to nonintuitive halide-dependent shifts in the emission band energies. A similar treatment might well prove to be valid for the $Cu_4X_4(pdmp)_4$ series.

III. Other Cuprous Halide Complexes

By far the most quantitative photophysical attention has been paid to tetranuclear complexes; however, numerous cuprous halide complexes ranging from the mononuclear species to long chain polymers are luminescent under specified conditions. Some of these species are listed in Table 5.[4,7,15,36−39] The photophysics of mononuclear complexes have been reviewed recently[6,40,41] and will not be discussed in detail here. However, when such species demonstrate luminescence, the emissive excited states are likely to have orbital parentage as either metal-centered d^9s^1 or MLCT excited states. The former is the suggested assignment for the surprising room temperature emissions observed for CuX salts in concentrated NaX solutions based on the relative insensitivity of emission maxima (475, 465, and 493 nm for X = Cl, Br, and I, respectively) but not lifetimes to the nature of X.[6a] Alternatively, structurally well-defined Cu(I) complexes with sterically demanding bidentate polyaromatic amines such as 2,9-dimethyl-1,10-phenanthroline (dmp) show strong visible range absorption bands and emissions consistent with a MLCT assignment both in solution (e.g., λ_{max}^{em} = 730 nm in 298 K dichloromethane) and in the solid state at various T.[6b] Other well-defined complexes such as $Cu(py)_3I$ and salts of CuL_4^+ (L = py or acetonitrile)

only emit as solids or in low-temperature glasses (e.g., solid $[Cu(py)_4]PF_6$ emits at 525 nm at 298 K), and the similarities of emission band shapes, energies, and lifetimes as well as the results of ab initio calculations point to emission from a common d^9s^1 ES in these cases.[40,41]

When solutions of $Cu_4I_4py_4$ are exposed to a large excess of pyridine, the dinuclear complex $Cu_2I_2py_4$ is formed which, when isolated as a solid, gives emission at ambient and lower T (λ_{max}^{em} = 517 and 510 nm, respectively).[7,41] Similar luminescence was observed for the dinuclear complex $Cu_2I_2(Et_4en)_2$ of the aliphatic amine Et_4en = *N*,*N*,*N*′,*N*′-tetraethylethylenediamine), so one must conclude that ligand orbitals are not involved. Given that d_{CuCu} for $Cu_2I_2py_4$ (2.70 Å)[42] is comparable to that seen in **A**, orbitals delocalized between the two metal centers are likely to play a role in the excited states. However, the emission bands observed are not significantly different in energy from those seen in related mononuclear systems, so it is not clear what importance such delocalization has in this case. Li et al. examined the emission spectra of open chain trinuclear copper(I) complexes with the bridging tridentate phosphine and bridging halide ligands of the type $[Cu_3(DPMP)_2(MeCN)_2(\mu\text{-}X)_2]ClO_4$ (X = Cl or I, DPMP = bis(diphenylphosphinomethyl)phenylphosphine, i.e., $(Ph_2PCH_2)_2PPh$).[37] The insensitivity of the emission energy to the identity of X was interpreted as suggesting no significant XLCT or XMCT contribution to the emission excited states. (However, the qualification with regard to changes in halide ionicities discussed above still applies.) Instead, these were assigned as predominantly MC (d−s) states since the crystal structures indicated long Cu−Cu distances (∼3.3 Å). These ES proved to be potent reductants undergoing oxidative quenching by *N*-ethylpyridinium ion to give a transient absorption band at 400−550 nm attributed to a mixed-valent copper cluster (eq 8).[37]

$$[Cu_3(DPMP)(MeCN)_2(\mu\text{-}X)_2^{+}]^* + Q^+ \rightarrow Cu_3(DPMP)(MeCN)_2(\mu\text{-}X)_2^{2+} + Q \quad (8)$$

$$Q^+ = N\text{-ethylpyridinium ion}$$

At the other end of the nuclearity scale is the polymeric species $(CuIpy)_\infty$, with the ribbonlike stair-step structure illustrated in Figure 1.[4] As a solid, $(CuIpy)_\infty$ shows a single emission band at a wavelength (λ_{max}^{em} = 437 nm) similar to the HE band of $Cu_4I_4py_4$ and like that band shows only modest thermochromism.[4,7] The d_{CuCu} distances (2.9 Å) in the polymeric form are longer than those in the cubane isomer $Cu_4I_4py_4$. As a result, the ^{3}CC excited state, which involves delocalization of the LUMO over several metal centers, is likely to be destabilized, so the polymer emission was assigned to a ^{3}XLCT excited state.[7]

A closely related polymer has been shown to demonstrate an interesting response to the vapors of volatile organic compounds (VOCs). Cariati et al.[38] have found that the polymeric solid $\{CuI(4\text{-picoline})\}_\infty$, which is characterized by a room temperature blue emission, is transformed into the corresponding cubane isomer by exposure to toluene vapor at ambient room temperature. The luminescence spectrum is dominated by a bright yellow solid-state emission characteristic of the cubane cluster $Cu_4I_4(4\text{-picoline})_4$. The process is reversed by exposing the new material to pentane vapors. While the vapochromic luminescence response of these cuprous iodide materials has potential in terms of developing VOC sensors, the system reported was too slow to be practical in this regard.

The crystal structure and luminescent behavior of another cuprous halide polymer $[(Ph_3P)_2Cu_2(\mu\text{−}Cl)_2(\mu\text{-pyrazine})]_\infty$ (d_{CuCu} = 3.059 Å) have been reported by Henary et al.[39] At low temperature (20 K), the solid-state emission spectrum displays a band at 612 nm. The presence of three ligand types, bridging chloride and pyrazine plus terminal triphenylphosphine, led to some interesting ambiguity as to contributions of the ligand orbitals to the excited state. However, resonance Raman studies established that the pyrazine ligands were most perturbed by the lowest electronic excitation.[39] On the basis of these data, the emission was attributed to a copper(I) to pyrazine ^{3}MLCT charge transfer state. On the other hand, it should be noted that the same data would not be inconsistent with a ^{3}XLCT assignment.

IV. Polynuclear Cu(I) and Ag(I) Complexes with Chalcogen Ligands

Cuprous and other d^{10} coinage metal ions readily form luminescent polynuclear complexes with chalcogenide ligands. Among these are some excellent opportunities to compare structurally analogous copper(I) and silver(I) clusters, examples being the hexanuclear Cu(I) and Ag(I) complexes $M_6(mtc)_6$ (mtc^- = di-*n*-propylmonothiocarbamate) with a nearly octahedral arrangement of the six metal centers (Figure 9). For the limited number of examples where such comparisons can be made, the silver(I) clusters emit at higher energy than the copper(I) homologues but are significantly less emissive, especially at ambient temperature. Some photophysical properties of these and several other Ag(I) and Cu(I) clusters with chalcogenide ligands are reported in Table 6.[43−50]

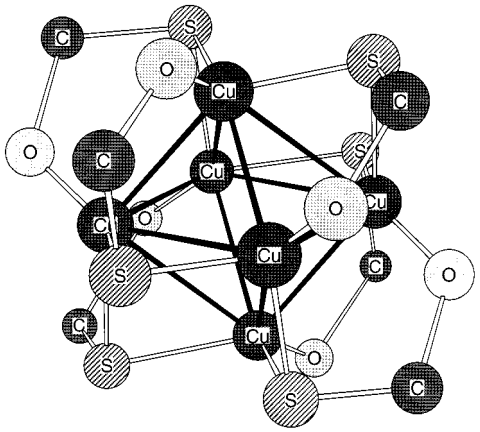

Figure 9. Illustration of $Cu_6(mtc)_6$ structure showing the Cu_6 octahedron with six edges bridged by the sulfur atoms from the di(*n*-propyl)monothiocarbamate (mtc) ligands. For clarity, the $-N(n\text{-}Pr)_2$ group on each of the six carbon atoms is not shown.

Table 6. Emission Maxima and Lifetimes of Cu(I) and Ag(I) Clusters with Chalcogenide Ligands in Various Media

cluster	medium	T (K)	λ_{max}^{em} (nm)	λ_{max}^{ex} (nm)	τ_{em} (μs)	ref
$Cu_6(mtc)_6$	solid	294	706	~400	1.0	43
	solid	77	767	~400	14	
	toluene	294	725	351	1.0	
	toluene	77	762	357	20	
$Ag_6(mtc)_6$	solid	77	644	360, 390	83, 109	43
	toluene	77	607	325, 359	131	
$Ag_6(dtc)_6$	solid	77	545	430, 455	8.4	43
	toluene	294	550	431	21	
$[Cu_5(SPh)_7][NMe_4]_2$	solid	298	615	430		44
		77	628	426		
	CH_3CN	298	660	350	3.1	
		77	661	365	36	
$[Cu_4(SPh)_6[NMe_4]_2$	solid	298	576	425	11	44
		77	584	426	52	
$[Cu_5(SAd)_6][NEt_4]$	solid	140	618			45
$[(C_6H_5)_4P]_2[Cu_7(C_2H_5S)_8]$	solid	298	591			46
$[(C_6H_5)_4P]_2[Cu_4(C_2H_4S)_6]$	solid	223	665			46
$[Cu_4(\mu\text{-dppm})_4(\mu_4\text{-S})][PF_6]_2$	solid	298	579		3.6	47a
		77	606			
	MeCN	298	618		7.8	
	Pr^nCN	77	539, 610 sh			
$[Cu_4(\mu\text{-dppm})_4(\mu_4\text{-Se})][PF_6]_2$	solid	298	595		3.9	47b
		77	619			
	MeCN	298	622		6.9	
	Me^2CO:MeOH:EtOH	77	478, 608			
$[Ag_4(\mu\text{-dppm})_4(\mu_4S)][CF_3SO_3]_2$	solid	298	516		1.0	47c
		77	536			
$[Ag_4(\mu\text{-dppm})_4(\mu_4\text{-Se})][CF_3SO_3]_2$	solid	298	527		0.9	47c
		77	552			
	MeCN	298	572		3.4	
$[Ag_4(\mu\text{-dppm})_4(\mu_4\text{-Te})][CF_3SO_3]_2$	solid	298	574		3.1	47c
		77	588			
	MeCN	298	626		3.3	
$[Cu_4(\mu\text{-dtpm})_4(\mu_4\text{-S})][PF_6]_2$	solid	298	604		3.5	47d
		77	658			
	MeCN	298	620		7.7	
$[Cu_4(N,N'$-1,4-butanebis(1,3-dimethyl-4-iminomethyl-5-thiopyrazole)$_2]$	solid	298	594		10.5	48
		77	610		30	
	toluene	298	594		1.9	
		77	600		39	
$[Cu_4(N,N'$-1,4-butanebis(3-methyl-1-phenyl-4-iminomethyl-5-thiopyrazole)$_2]$	solid	298	540		0.69	48
		77	542		101	
	toluene	298	602		0.74	
		77	602		40	
$[Cu_4(N,N'$-1,4-butanebis(1,3-diphenyl-4-iminomethyl-5-thiopyrazole)$_2]$	solid	298	588		3.1	48
		77	616		30	
	toluene	298	604		5.4	
		77	611		44	
$[Cu_4(N,N'$-(2,2′-diphenyl)bis(1,3-diphenyl-4-iminomethyl-5-thiopyrazole)$_2]$	solid	298	599		2.8	48
		77	597		54	
	toluene	298	626		0.18	
		77	616		51	
$[Cu_4(N$-(2,6-dimethylphenyl)-3-methyl-1-phenyl-4-iminomethyl-5-thiopyrazole)$_2]$	solid	298	594		1.2	48
		77	608		42	
	toluene	298	593		0.098	
		77	595		61	
$[Cu_4(N$-(2-propyl)-1,3-diphenyl-4-iminomethyl-5-thiopyrazole)$_2]$	solid	298	546		1.5	48
		77	548		77	
	toluene	298	620		0.018	
		77	680		114	
$[Cu(SC_6H_4\text{-}2\text{-}CH_2NMe_2)]_3\cdot THF$	solid	4.2	480	350		49
			610	400		
$[Cu(SC_6H_5\text{-}2\text{-}CH(Me)NMe_2]_3\cdot THF$	solid	4.2	555	400	350	49
					6.0 (298 K)	
$[Cu_3(dppm)_3(WS_4)]$	solid	298	440, 615		2.8	50
	solid	77	615			

The $Cu_6(mtc)_6$ cluster displays a deep orange luminescence (λ_{max}^{em} = 706 nm) as an ambient temperature solid, and this shifts to the red when cooled to 77 K (767 nm).[43] While both $Ag_6(mtc)_6$ (644 nm) and $Cu_6(mtc)_6$ are brightly emissive as solids and in frozen solutions at 77 K, only the latter is luminescent from ambient temperature fluid solutions or solids. The lowest energy absorption bands occur at λ_{max}^{abs} = 360 and 430 nm, respectively, in room temperature toluene solutions.

Possible assignments for the luminactive excited states are ones originating from ligand-centered $\pi-\pi^*$ (LC) transitions, from metal- (or cluster) centered d → s transitions, or from either MLCT or ligand to metal charge transfer (LMCT) transitions. Of these the LC assignment does not appear likely,

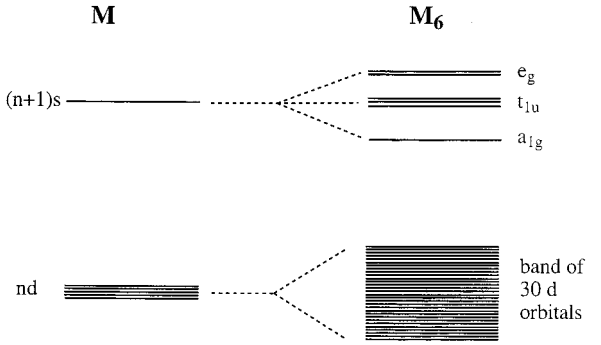

Figure 10. Splitting of the frontier metal orbitals in the formation of the M_6 octahedral cluster.

since free ligand mtc^- absorption bands are quite high in energy ($\lambda_{max}^{abs} < 200$ nm) and Na[mtc] does not display any visible range emission.[43] Similarly, while MLCT excited states are important in the photophysical properties of the copper(I) complexes of easily reducible ligands such as phenanthroline,[6b] the π^* orbitals of mtc^- are too high in energy to serve as acceptor orbitals for low-lying MLCT states.

These considerations leave LMCT and metal-centered (d−s) ES as the most likely assignments for the luminactive state. The electron affinities of the free Cu^+ and Ag^+ ions are comparable.[51] Thus, to a first approximation, LMCT transitions of analogous Cu(I) and Ag(I) complexes might be expected to have comparable energies, although the energies of frontier molecular orbitals would certainly be dependent on the extent of mixing due to metal−metal and metal−ligand covalent interactions. The optical electronegativities of thiocarbamato ligands (2.7)[52] are just a bit higher than of iodide (2.5).[53] Given that the thiocarbamate complexes of more oxidizing metal ions such as Cu(II) or Ag(II) are strongly colored owing to LMCT absorption bands in the visible,[54] it is reasonable to speculate that the analogous LMCT absorptions for the Cu(I) and Ag(I) clusters occur in the near-UV region of the spectrum. Alternatively, MC states are also reasonable candidates given that d → s absorptions of the free ions $Cu^+(g)$ and $Ag^+(g)$ occur at relatively low energies (21.9×10^3 and 39.2×10^3 cm^{-1}, respectively, for the lowest energy spin forbidden transitions).[55] The appearance of both the longest wavelength absorption band and the emission band for $Cu_6(mtc)_6$ at somewhat lower energies than for the respective bands of $Ag_6(mtc)_6$ is consistent with this trend, but the differences are much smaller. The effect of metal−metal interactions in the $(M^I)_6$ octahedra would lead to substantial splitting of the d and, especially, s orbitals in a manner which may lead to marked effects on the expected HOMO and LUMO energies (Figure 10). It is likely that the metal−metal interactions in $Ag_6(mtc)_6$ are substantially greater than in $Cu_6(mtc)_6$ because, relative to the sums of their respective van der Waals radii, 3.4 and 2.8 Å, respectively, the Ag−Ag distances (d_{AgAg} = 2.94−3.28 Å) are effectively shorter than the Cu−Cu distances (d_{CuCu} = 2.70−3.06 Å).[56] Such considerations as well as comparisons to the iodide clusters noted above led to assignment of the luminactive state in both $Ag_6(mtc)_6$ and $Cu_6(mtc)_6$ as a cluster-centered excited state of mixed ^{3}{LMCT/(d−s)} character.[43] The higher energy emission for $Ag_6(mtc)_6$ can be correlated to the higher d → s energy for the free metal ion, moderated in part by greater mixing of the metal orbitals in the Ag^I_6 cluster.

Yam et al.[47] have described a particularly interesting series of tetranuclear Cu(I) and Ag(I) chalcogenide clusters $[M_4(\mu\text{-dppm})_4(\mu_4\text{-E})]^{2+}$ with E = S or Se for M = Cu and E = S, Se, or Te for M = Ag where dppm = bis(diphenylphosphino)methane. Unlike the tetrahedral nature of the Cu_4 clusters described above, the structures of these ions are based upon M_4E^{2+} tetragonal pyramids with the four metal ions occupying the basal plane and the chalcogenide ion E^{2-} at the apex. The absorption spectra of these all show a high-energy shoulder at ∼240−260 nm attributed to an intraligand (dppm) transition and a lower intensity tail in the 350−450 nm region. The PF_6^- salts are all luminescent as solids at 298 and 77 K and follow the pattern noted above, i.e., the Ag(I) cluster emission bands occur at higher energies than their Cu(I) homologues (Table 6). Also notable is the shift to lower energy of the emission bands with a change in E from S to Se to Te. Furthermore, measurements on 298 K acetone solutions clearly show the emission quantum yields to be 1−2 orders of magnitude higher for the copper compounds. Molecular orbital calculations[47d] conclude that the HOMO in these M_4E^{2+} complexes is mainly of M−E bonding character while the LUMO is largely metal-centered with the HOMO−LUMO gap decreasing along the series S > Se > Te. Thus, on the basis of arguments analogous to those presented above for the $Cu_4I_4L_4$ cubane and the $M_6(mtc)_6$ clusters, Yam and co-workers concluded that the emitting state of the M_4E^{2+} cluster complexes is also a ^{3}CC type state constituted from a mixture of LMCT ($E^{2-} \rightarrow M^I_4$) and MC (d → s) configurations.[47]

Copper clusters based upon various thiolate ligands occur in a wide variety of metal:ligand compositions. Dance and other researchers have developed a series of Cu(I)−thiolate clusters, demonstrating the wide structural variety of these complexes.[57] Of these, two, $Cu_5(SPh)_7^{2-}$ and $Cu_4(SPh)_6^{2-}$, were studied briefly by Bourassa.[44] Both proved to be brightly luminescent at room temperature in the solid state (Table 6). Deep orange crystals of $[NMe_4]_2[Cu_5(SPh)_7]$ gave a bright orange-red emission as a room temperature solid (λ_{max}^{em} = 615 nm) and in ambient temperature acetonitrile solution (660 nm, Figure 12), while the yellow crystals of $[NMe_4]_2[Cu_4(SPh)_6]$ showed green luminescence at ambient temperature (576 nm). Like many of the other cuprous clusters, these displayed large Stokes shifts from the excitation maximum to the emission maximum, especially in solution (Table 6).

The luminescent behavior of the cyclic trinuclear compounds $(CuSAr)_3$ and $(CuSAr')_3$ (Ar = SC_6H_4[(R)-CH(Me)NMe_2]-2, Ar′ = $C_6H_4(CH_2NMe_2)$-2) has been examined by Knotter et al.[49] These compounds have an interesting chair conformation for the six-membered $(CuS)_3$ ring which makes up the core of the clusters and relatively short d_{CuCu} values of 2.83 Å. An unusual feature was the bright triboluminescence observed upon breaking the crystals of the chiral

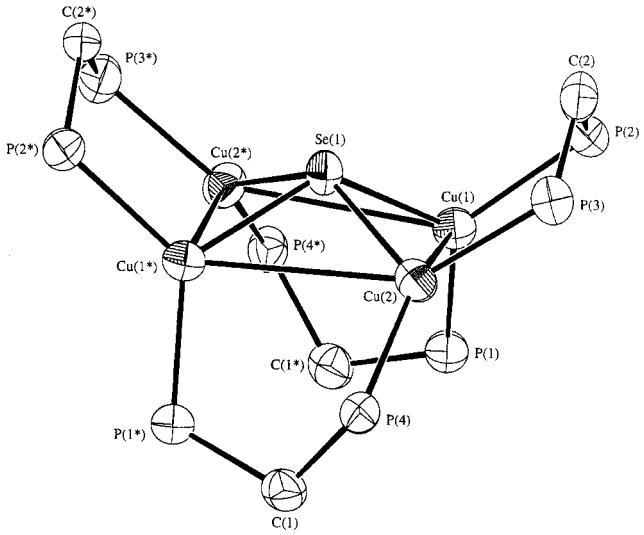

Figure 11. Representation of key structural elements of the $Cu_4(\mu\text{-dppm})_4(\mu^4\text{-Se})]^{2+}$ cation (dppm = bis(diphenylphosphino)methane) (illustration provided by V. W.-W. Yam. (Reprinted with permission from ref 47b. Copyright 1996 American Chemical Society.)

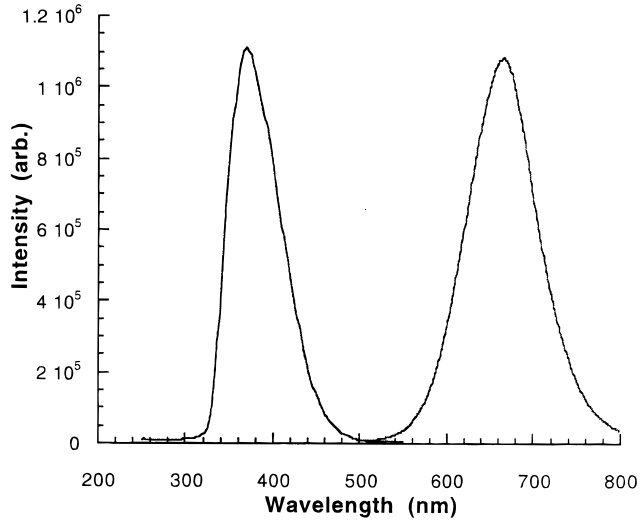

Figure 12. Emission and excitation spectra of 10 mM $[NMe_4]_2[Cu_5(SPh)_7]$ in 298 K CH_3CN solution. (Reprinted with permission from ref 44. Copyright 1998.)

compounds containing SAr′. The luminescence spectrum of solid $[CuSAr]_3$ at liquid helium temperature gave a broad featureless band at 555 nm with an excitation maximum at 400 nm, while solid $[CuSAr']_3$ displayed two bands with distinct excitation profiles (λ_{max}^{em}(i) = 480 nm, λ_{max}^{ex}(i) = 350 nm, λ_{max}^{em}(i) = 610 nm, λ_{max}^{ex} (i) = 350−400 nm at 4.2 K). These emissions were suggested to originate from LMCT states in accord with the electron-donating ability of the thiolate ligands. The occurrence of two emission bands in the spectrum of $(CuSAr')_3$ was attributed to individual copper centers having different orientations of the aryl thiolates, leading to three-electron−two-sulfur bonds in the lower energy ES.[49] However, it is not clear to the reviewers why these very similar complexes have such different photophysical behaviors.

A. Dynamic Quenching Studies.

Two of the chalcogenide clusters discussed above, $Cu_5(SPh)_6^{2-}$ (**B**) and $Cu_4(\mu\text{-dppm})_4(\mu_4\text{-Se})^{2+}$ (**C**), have been subjects of emission quenching studies similar to those for the $Cu_4I_4py_4$ cluster **A**. Second-order k_q values were determined from linear Stern−Volmer plots for quenching emission from toluene solutions of $[NMe_4]_2[Cu_5(SPh)_6]$ by various aromatic organic and Cr(III) tris(β-diketonate) compounds[44] and from acetone solutions of $[Cu_4(\mu\text{-dppm})_4(\mu_4\text{-Se})](PF_6)_2$ by a series of substituted methyl- and ethylpyridinium salts.[47] With the exception of some of the Cr(III) complexes which have a low-lying excited state (^2E_g, $E \approx 1.28\ \mu m^{-1}$) and may quench the luminescent ES of **B** (est. E^{00} 1.73 μm^{-1}) by energy transfer, the other quenchers of **B** and all those used to study **C** must operate via an electron transfer mechanism. In this context, fits of the quenching data for these two complexes according to eq 6 gave typical values for $v_n\kappa_e$ but large reorganization energies (λ) for quenching of **B** (1.6 eV) and of **C** (1.12 eV).[44,47] Results of several such redox quenching studies of cuprous cluster emissions are summarized in Table 7.

B. Copper(I) in Metallothionein Proteins.

That copper(I) binds facilely with chalcogen ligands is reflected by its uptake by metallothionein proteins such as apo-MT-2 (metallothionein protein isoform 2, obtained from rabbit liver) which has 20 thiolate groups along its peptide chain available for binding metals.[58] Stillman and co-workers have demonstrated that apo-MT-2 when titrated with Cu(I) as $Cu(CH_3CN)_4^+$ gave a strong blue emission (λ_{max}^{em}(uncorrected) = 535 nm in frozen 77 K solution) that increased in intensity to a maximum as the metal/protein ratio was increased to 12. An excitation maximum around 300 nm was also determined, showing the typical large Stokes shift. Such emissions in the 550−650 nm region with nanosecond to microsecond lifetimes appear to be a general property of copper-containing metallothioneins.[58c] Although these photophysical properties have been attributed to metal-centered excited states,[58c] a more delocalized CC type description, as used for the various cuprous chalcogen clusters described above, would also be consistent.

The emission from Cu(I)−MT-2 complexes is dynamically quenched by solution dioxygen ($k_q \times 10^9$ $M^{-1}\ s^{-1}$) without observable alteration of the solution CD spectrum.[59] This suggests that oxygen is serving to quench via energy transfer without significant oxidation of the ground state, and this and other properties were used to argue that the luminescent excited state is of triplet character. The presence of ferricyanide led to oxidative quenching of the Cu_{12}-MT emission and concomitant disruption of the protein three-dimensional structure.

Analogous experiments using Ag(I) (in the form of $AgNO_3$) as the titrant produced a greenish emission at 77 K centered at 570 nm, which reached an intensity maximum when 12 equiv of Ag^+ were added per apo-MT 2 molecule.[58a]

Similar luminescent behavior was exploited by Weser to examine the metal binding behavior of the

Table 7. Reorganization Energy and Excited State Reduction Potentials from Oxidative Luminescence Quenching Studies

cluster[a]	$E_{1/2}(X^+/X^*)$ (eV) [b]	λ (eV)[c]	Stoke's shift (μm^{-1})[d]	ref
$Cu_4I_4py_4$	−2.25	1.86	1.63	31
$Cu_5(SPh)_7^{2-}$	−2.70	1.60	1.34	44
Cu_4L_2	−2.31	1.37	1.26	48
$Cu_4(\mu\text{-dppm})_4(\mu_4\text{-Se})^{2+}$	−1.55	1.12		47b
$[Cu_4(\mu\text{-dppm})_4(\mu_4\text{-}\eta^1,\eta^2\text{-C}\equiv\text{C}-)]^{2+}$	−1.77	1.39		67
$[Cu_4(PPh_3)_4(\mu_3\text{-}\eta^1,\eta^1,\eta^2\text{-C}\equiv\text{CC}_6\text{H}_4\text{OMe}-p)_3]^+$	−1.71	1.36		68

[a] Cu_4L_2 = [Cu_4 (*N,N′*-1,4-butanebis(1,3-dimethyl-4-iminomethyl-5-thiopyrazole)$_2$]. [b] Versus SSCE. [c] Reorganization energy term determined from a fit of quenching rate constants according to eq 6. [d] Stokes shift calculated from $\nu_{max}^{ex} - \nu_{max}^{em}$.

apo-MT-2 and the α and β fragments of the rat liver MT-2.[60] Photoluminescence experiments in conjunction with circular dichroism and UV−vis absorption studies were used to examine the Cu(I) binding ability of the apo-MT-2 intact metallothionein, the α and β fragments separately, and the α and β fragments together. The β fragment emits at 595 nm at room temperature when Cu(I) is present, and the emission intensity shows a linear increase with increasing Cu(I) equivalents to a maximum at six equivalents. The α fragment displays emission at 615 nm upon binding Cu(I), the intensity of which increases until saturating at six copper equivalents. In this case, apo-MT-2 showed emission at 610 nm which reached a maximum at 12 copper equivalents added. Circular dichroism was able to reveal two distinct phases of cuprous incorporation into the protein; two distinct sets of spectral changes split into the first and second sets of six copper ions.

The temperature dependence of the luminescence properties of Cu(I) MT-2, coupled with examination of the CD spectra, revealed information on the modes of binding of Cu(I) to MT-2.[61] It was found that the α domain emitted much more intensely than its β counterpart in MT-2. While initial copper binding proved to be statistical for 1−6 equivalents (i.e., there is no cooperativity), there was later rearrangement to bind preferentially in the β domain with concurrent loss in emission intensity. At Cu(I)/protein loading approaching 12, the luminescence intensity increased dramatically, which was interpreted to indicate rearrangement of the protein backbone to give a specific, tightly structured Cu_{12}MT-2 site that efficiently excludes solvent and correspondingly is much more luminactive.

V. Cuprous Clusters with Acetylide Ligands

The photoluminescence properties of a class of multinuclear alkynylcopper(I) complexes has been the subject of study by Yam and co-workers.[62−72] These compounds display several acetylide bonding modes and a diversity of polynuclear copper(I) structures as illustrated in Figure 13. Aspects of their photophysical properties are summarized in Table 8.

An early study was concerned with the trinuclear complexes $Cu_3(dppm)_3(\mu_3\text{-}\eta^1\text{-C}\equiv\text{C}^t\text{Bu})(\mu_3\text{-Cl})]PF_6$ and $Cu_3(dppm)_3(\mu_3\text{-}\eta^1\text{-C}\equiv\text{CR})_2]PF_6$ (R = ^{t}Bu, Ph).[65] In the solid state, all three complexes display two emission bands at 77 K, one at 440−485 nm, and a less intense band at 525−540 nm. Comparison of the emission energies for the ^{t}BuC≡C− complexes to those of the PhC≡C compounds led to the assignment of the high-energy emission as due to a MLCT [Cu → p*(−C≡CR)] excited state. From the long lifetimes of the low-energy band for all complexes and the lack of dependence upon the nature of the acetylide ligand, it was proposed that this emission be assigned to a spin forbidden transition from a triplet metal-centered (d−s) state. Further studies have probed solventochromic shifts in these compounds' luminescence spectra.[64] The lower energy emission bands were noted to blue shift upon changing the solvent from acetonitrile to acetone. Furthermore, the lower energy emission of $Cu_3(dppm)_3(\mu^3\text{-}\eta^1\text{-C}\equiv\text{C}^t\text{Bu})]^{2+}$ (which is more easily reduced than the monocation analogues) was found at significantly lower energies (λ_{max} = 627 nm) than for those complexes. These data led to the proposal of a luminactive excited state with ^{3}LMCT character (RC≡C− → Cu_3) mixed with the ^{3}MC state. The red shift observed upon comparing the solution emission spectra with those obtained in the solid state was rationalized by proposing greater structural rearrangement in solution. The s-orbitals which would be the acceptor orbitals in either a LMCT or a MC transition have Cu−Cu bonding properties, and population of these would result in a structurally contracted excited state. This was emphasized in the context of the large Stokes shifts found for these systems.[70]

That the excited state cuprous acetylide clusters can serve as strong reducing agents was demonstrated in a study which examined redox quenching by various electron-acceptor pyridinium compounds.[64,71] For example, Stern−Volmer quenching plots gave a k_q of 6.9×10^9 M^{-1} s^{-1} for the reaction of $[Cu_3(dppm)_3(\mu_3\text{-}\eta^1\text{-C}\equiv\text{CPh})_2^+]^*$ with 4-(methoxycarbonyl)-*N*-methylpyridinium ion in degassed acetone. Time-resolved optical absorption studies revealed the production of pyridinyl radicals at 400 nm as well as a low-lying absorption at 810 nm assigned to an intervalence transition of a mixed-valence Cu^I-Cu^ICu^{II} complex (Figure 14). The time evolution of these bands demonstrated that back electron transfer rates to reform the starting materials is nearly diffusion-limited ($k_{bet} > 10^{10}$ M^{-1} s^{-1}).

The photophysical properties of other cuprous acetylide clusters followed a similar behavior (Table 8), and the lowest energy luminactive excited states can be consistently attributed to cluster-centered triplet excited states with mixed LMCT/MC character. The dynamic redox quenching of such ^{3}CC states for several clusters was investigated using a system-

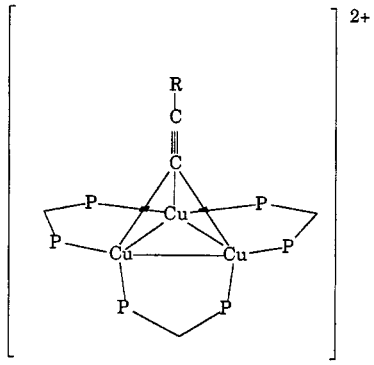

1: R = Ph
2: R = ^{t}Bu

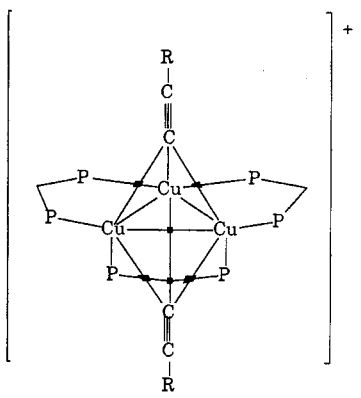

3: R = Ph
4: R = ^{t}Bu

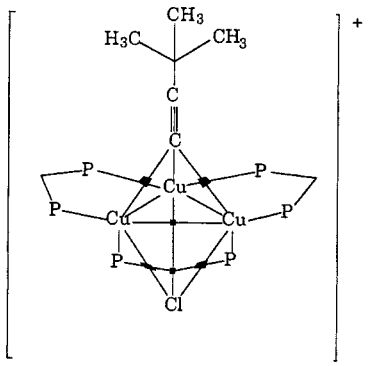

5

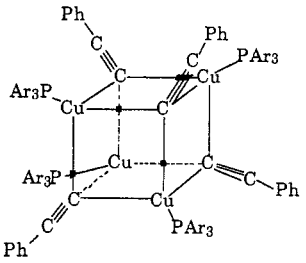

6: Ar = Ph
7: Ar = C_6H_4-F-*p*
8: Ar = C_6H_4-Me-*p*
9: Ar = C_6H_4-OMe-*p*

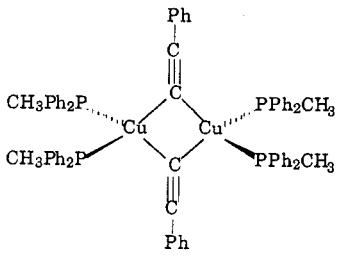

10

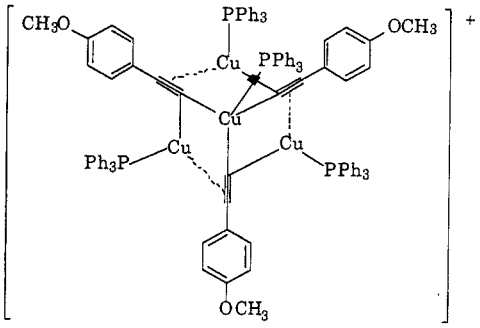

11

Figure 13. Examples of structural types of cuprous acetylide polynuclear complexes. (Figure adapted from drawings provided by V. W.-W. Yam.)

atic series of pyridinium ion quenchers with different reduction potentials, each having lowest $\pi\pi^*$ states too high for an energy transfer mechanism to be important. Analysis of the quenching rates as functions of $E_{1/2}(Q/Q^-)$ according to electron transfer theory, as described above, gave, in each case, large values for the electron transfer reorganization energy term λ, an observation which can be interpreted in terms of the substantial distortions of the CC excited state owing to enhanced metal−metal bonding relative to ground state configurations. The large Stokes shifts between excitation and emission maxima may also be attributed to such distortions. Values of λ calculated for several cuprous clusters are summarized in Table 7.

The analogous monocapped and bicapped silver acetylide clusters $Ag_3(\mu\text{-dppm})_3(\mu_3\text{-}\eta^1\text{-}C{\equiv}CC_6H_4R)^{2+}$ and $Ag_3(\mu\text{-dppm})_3(\mu_3\text{-}\eta^1\text{-}C{\equiv}CC_6H_4R)_2^{+}$ have also been prepared for various substituents R, and several have been characterized by X-ray crystallography.[73] The solids are luminescent at 298 and 77 K, but the solutions are emissive only at 77 K. Microsecond

Table 8. Examples of Copper(I) Clusters with Acetylide Ligands

compound	medium	T (K)	λ_{max}^{em} (nm)	τ_{em} (μs)	ref
$[Cu_2(PPh_2Me)_4(\mu\text{-}\eta^1\text{-}C{\equiv}CPh)_2]$	CH_2Cl_2	298	529, 660 sh		62
	solid	298	467, 509		
	solid	77	464, 511	87	
$[Cu_3(\mu\text{-}^n\text{PrPNP})_3(\mu_3\text{-}\eta^1\text{-}C{\equiv}CC_6H_4OEt\text{-}p)_2]BF_4$	Me_2CO	298	467	4.4	63
	solid	298	459	3.1	
	solid	77	453 sh, 482		
	MeOH/EtOH (1:4 v/v)	77	445, 478		
$[Cu_3(\mu\text{-}^n\text{PrPNP})_3(\mu_3\text{-}\eta^1\text{-}C{\equiv}CC_6H_4Ph\text{-}p)_2]BF_4$	Me_2CO	298	516, 554, 615 sh	26.1	63
	solid	298	521, 558 sh, 615 sh	6.6	
	solid	77	522, 565, 615 sh		
	MeOH/EtOH	77	510, 546, 615 sh		
$[Cu_3(\mu\text{-}^n\text{PrPNP})_3(\mu_3\text{-}\eta^1\text{-}C{\equiv}CPh)_2]BF_4$	Me_2CO	298	465	3.4	63
	solid	298	461	4.0	
	solid	77	459, 485, 495, 507		
	MeOH/EtOH	77	445, 479		
$[Cu_3(\mu\text{-}^n\text{PrPNP})_3(\mu_3\text{-}\eta^1\text{-}C{\equiv}CC_6H_4\text{-}NO_2\text{-}p)_2]BF_4$	Me_2CO	298	454	1.6	63
	solid	298	400	4.0	
	solid	77	400		
	MeOH/EtOH	77	453, 671		
$[Cu_3(\mu\text{-}^n\text{PrPNP})_3(\mu_3\text{-}\eta^1\text{-}C{\equiv}CtBu)_2]PF_6$	Me_2CO	298	464	3.2	63
	solid	298	459	1.0, 5.3	
	solid	77	485		
	MeOH/EtOH	77	474		
$[Cu_3(\mu\text{-}C_6H_5PNP)_3(\mu_3\text{-}\eta^1\text{-}C{\equiv}CC_6H_4OEt\text{-}p)_2]PF_6$	Me_2CO	298	484, 646	7.0	63
	solid	298	469	0.3	
	solid	77	493		
$[Cu_3\{\mu\text{-}(C_6H_4\text{-}CH_3\text{-}p)PNP\}_3(\mu_3\text{-}\eta^1\text{-}C{\equiv}C\text{-}C_6H_4OEt\text{-}p)_2]PF_6$	Me_2CO	298	464, 632	2.5	63
	solid	298	466, 550 sh	4.8	
	solid	77	491		
$[Cu_3\{\mu\text{-}(C_6H_4\text{-}F\text{-}p)PNP\}_3(\mu_3\text{-}\eta^1\text{-}C{\equiv}C\text{-}C_6H_4OEt\text{-}p)_2]PF_6$	Me_2CO	298	470 sh, 623	6.4	63
	solid	298	467, 550 sh	6.6	
	solid	77	500		
$[Cu_3(\mu\text{-dppm})_3(\mu_3\text{-}\eta^1\text{-}C{\equiv}CPh)][BF_4]_2$	Me_2CO	298	499	6.8	64
	solid	298	500	21	
	solid	77	492, 530 s		
$[Cu_3(\mu\text{-dppm})_3(\mu_3\text{-}\eta^1\text{-}C{\equiv}C^tBu)][PF_6]_2$	Me_2CO	298	640	2.6	64
	solid	298	627	14	
	solid	77	450, 570 sh, 692		
$[Cu_3(\mu\text{-dppm})_3(\mu_3\text{-}\eta^1\text{-}C{\equiv}CPh)_2]PF_6$	Me_2CO	298	495	5.9	64, 65
	solid	298	493	14	
	solid	77	485, 525 sh		
	Pr^nCN glass	77	471, 500 sh		
$[Cu_3(\mu\text{-}Ph_2PCH_2PPh_2)_3(\mu_3\text{-}\eta^1\text{-}C{\equiv}CC_6H_4C{\equiv}C\text{-}p)Cu_3(\mu\text{-}Ph_2PCH_2PPh_2)_3][BF4]$	CH_2Cl_2	298	596	40	66
	solid	298	583	222	
	solid	77	583		
	EtOH/MeOH	77	579		
$[Cu_4(\mu\text{-dppm})_4(\mu_4\text{-}\eta^1,\eta^2\text{-}C{\equiv}C)](BF_4)_2$	Me_2CO	298	562	16	67
	solid	298	509	9.8	
	solid	77	551		
$[Cu_4(PPh_3)_4(\mu_3\text{-}\eta^1,\eta^1,\eta^2\text{-}C{\equiv}CC_6H_4OMe\text{-}p)_3]^+$	Me_2CO	298	675	4.0	68
	solid	298	445, 630 sh	20.7	
	solid	77	445		
$[Cu_4(PPh_3)_4(\mu_3\text{-}\eta^1\text{-}C{\equiv}CPh)_4]$	CH_2Cl_2	298	420, 520 sh, 616	3.6	69
	solid	298	483 sh, 522	3.7	
	solid	77	477, 524		
$[Cu_4\{P(C_6H_4F\text{-}p)_3|_4(\mu_3\text{-}\eta^1\text{-}C{\equiv}CPh)_4]$	CH_2Cl_2	298	420, 510 sh, 606	0.86	69
	solid	298	516	1.3	
	solid	77	516		
$[Cu_4\{P(C_6H_4Me\text{-}p)_3\}_4(\mu^3\text{-}\eta^1\text{-}C{\equiv}CPh)_4]$	CH_2Cl_2	298	410, 510 sh, 620		69
	solid	298	548	0.52	
	solid	77	535		

emission lifetimes were observed for the 298 K solids. The emission bands appeared at higher energy than those for the respective cuprous clusters, with blue shifts ($\sim$0.25 μm^{-1}) similar to those seen for the $M_6(mtc)_6$ clusters discussed above. The emission band of several Ag(I) clusters showed vibronic structure with progression spaced at $\sim$2000 cm^{-1} characteristic of the ν_{CC} stretch of the acetylide triple bond. The observation of vibrational progression indicates involvement of the acetylide unit in the luminactive excited state. As for the $M_6(mtc)_6$ clusters and the copper acetylide analogues, this excited state was concluded to be a triplet state with mixed {LMCT/(d−s)} character.

VI. Other Cuprous Polynuclear Systems

Photophysical studies have been carried out on a variety of other multinuclear copper(I) compounds, and some of these are listed in Table 9.[74−83] The first two entries are representatives of series of binuclear cuprous complexes described, respectively, by Kaim and co-workers[74] and by Yam and co-workers.[75] In the both cases, the two Cu(I) centers are bridged by

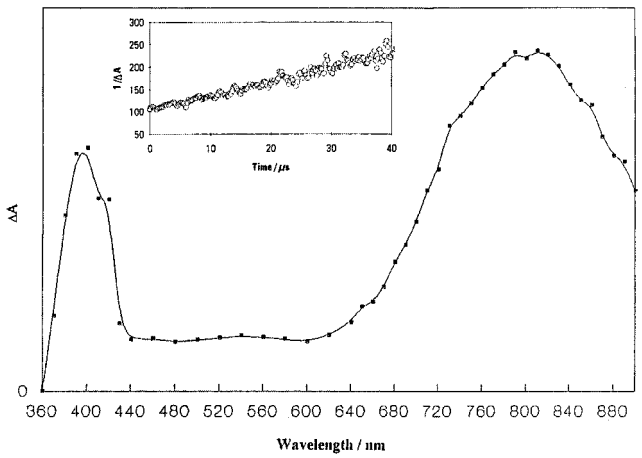

Figure 14. Time-resolved absorption spectrum of a solution of $Cu_3(dppm)_3(C{\equiv}CPh)_2]^+$ (0.05 mM) and 4-(methoxycarbonyl)-*N*-methylpyridinium hexafluorophosphate (13 mM) in degassed acetonitrile (0.1 M $^nBu_4NPF_6$) after laser flash photolysis. Inset: 1/ΔAbs versus time at 400 nm.

a polydentate aromatic nitrogen heterocycle in a manner such that there is no direct interaction between the two metals. Given the close analogy to the mononuclear $CuL_2(NN)^+$ (NN = substituted bipyridine or phenanthroline) complexes described earlier by McMillin,[6b] it is probable that the luminescence seen for both series finds its origin in metal to ligand charge transfer states. In the former series, bipyrimidine is the bridging ligand ([(μ-bipyrimidine)-$\{Cu(PR_3)_2\}_2]X_2$; R = C_6H_5, C_6D_5, *n*-$C_6H_4CH_3$; X = BF_4^-, PF_6^-, ClO_4^-) and strong solid-state emission was correlated with π−π stacking interactions between the bridging bipyrimidine and phenyl rings from the phosphine ligands. Only those structures with this feature displayed appreciable emissions. In the latter series, the bridging ligand was 2,3-bis(2-pyridyl)pyrazine (dpypz) or a derivative thereof ([$\{Cu(PPh_3)_2\}_2L]^{2+}$, L = dpypz, dmdpq, dpq, dcdpq, dpbq). For this series the energies of absorption and emission maxima for different ligands correlated well with the corresponding π_L* orbital energies, as estimated from experimental electrochemical studies. Such behavior is consistent with these transitions having MLCT character.[84]

Che and co-workers[78] examined the emission spectra of the dinuclear cuprous complex ions $[Cu_2(\mu\text{-}dppm)_2L_2)^{2+}$ (dppm = bis(diphenylphosphino)methane; L = 2MeCN, PPh_3, py, or various four-substituted pyridines). Again, these have relatively long copper−copper distances (~3.7 Å) so direct metal−metal interactions in the ground state are improbable. The λ_{max}^{em} values seen for these complexes fall near ~520 nm, just slightly red shifted from that of the free dppm ligand (500 nm), suggesting that the luminactive excited state in this case is largely a ligand localized ππ* excited state. However, it is notable that replacement of the labile acetonitrile ligands with the stronger donors PPh_3 or py leads to increases in the emission lifetimes and quantum yields by ~2 orders of magnitude, so it is clear that the metal center is playing an important role in the nonradiative deactivation pathways.

These and related compounds can also serve as photocatalysts for cleavage of alkyl halide C−X bonds and formation of C−C bonds.[78] Photolysis of the dinuclear compound $[Cu_2(\mu\text{-}dppm)_2(MeCN)_4]^{2+}$ (as well as its Au(I) analog) in the presence of alkyl halides such as benzyl chloride led to the photocatalytic cleavage of C−Cl bonds and formation of C−C bonds. This was accompanied by luminescence quenching, and transient absorbances attributed to the mixed-valence Cu^ICu^{II} intermediate were observed by time-resolved spectroscopy.[78a] The proposed mechanism involves direct halogen atom transfer from the alkyl halide to the excited state of the binuclear metal complex to give carbon radicals (eq 9). The latter subsequently dimerize.

Table 9. Luminescence Properties of Other Copper (I) Polynuclear Compounds

compound	medium	*T* (K)	λ_{max}^{em} (nm)	τ_{em} (μs)	ref
$[(\mu\text{-bpym})\{Cu(PPh_3)_2\}_2](BF_4)_2$	solid	298	630		74
	$CHCl_3$	298	758		
$[\{Cu(PPh_3)_2\}_2(dppyz)]_2^+$	solid	298	635		75
	CH_2Cl_2	298	650		
$[Cu(C_6H_5NNNC_6H_5)]_2$	solid	77	600	0.002	76
$[Cu_2\{\mu\text{-}(Ph_2P)_2py\}_3](PF_6)_2$	MeCN	298	400, 440		77
$[Cu_2(\mu\text{-}dppm)_2py_2][ClO_4]_2$	CH_2Cl_2	298	525	27	78
$[Cu_2(\mu\text{-}dppm)_2(MeCN)_4][ClO_4]_2$	CH_2Cl_2	298	530	0.4	78
$[Cu_2(\mu\text{-}dppm)_2(PPh_3)_2][ClO_4]_2$	CH_2Cl_2	298	550	75	78
$[Cu_2(dppm)_2(O_2CCH_3)]BF_4$	EtOH	77	440−600	68, 234	79
	solid	77	470		
$[Cu_2(\mu\text{-}^nPrPNP)_2(MeCN)_2](PF_6)_2$	solid	298	449	0.35	63
	solid	77	451		
$[Cu_2(\mu\text{-}C_6H_5PNP)_2(MeCN)_2](PF_6)_2$	solid	298	419, 500 sh		63
	solid	77	463, 530	0.20	
$[Cu_3(dppm)_3OH](BF_4)_2$	EtOH	298	540	89	80
	solid	77	510		
	EtOH	77	480	170	
$[CuN(SiMe_3)_2]_4$	CH_2Cl_2	300	512	30	81
	solid	77	524		
	Et_2O	77		690	
$[\{Cu(mes)\}_5]$	solid	298	644		62
	solid	77	653		
$[(CuPPh_3)_6L_2]$	solid	298	562	0.59	82
LH = trithiocyanuric acid	CH_2Cl_2	298	580	0.82	
$\{[Cu(dmb)_2]BF_4\}_n$	solid	77	490	39−289	83
	EtOH	77	548	46−352	

$$[Cu_2(\mu\text{-dppm})_2L_2]^{2+}* + RX \rightarrow \{[Cu_2(\mu\text{-dppm})_2\,L_2X]^{2+}, R^{\bullet}\} \quad (9)$$

The dinuclear 1,3-diphenyltriazide complex $Cu_2(PhNNNPh)_2$ (Figure 15) described by Harvey and co-workers[79] displays photophysical behavior different from all of the other polynuclear cuprous complexes described above. In this case, the emission band ($\lambda_{max}^{em} = 560$ nm) overlaps with the relatively low-energy excitation band ($\lambda_{max}^{ex} = 490$ nm), i.e., the Stokes shift is quite small.[79] In addition, the emission lifetime proved to be short ($\tau \cong 3$ ns at 77 K). On these bases, the emission was assigned to be fluorescence from a ligand-centered $\pi-\pi^*$ excited state localized primarily on the nitrogen frameworks mixed with some MLCT ($Cu_2 \rightarrow N_3$) character. Extended Hückel molecular orbital (EHMO) calculations as well as excited state vibrational spectroscopy were used to support this assignment. No phosphorescence was observed, and it was concluded that there was no evidence for Cu···Cu interactions despite the reported, very short, ground state d_{CuCu} value of 2.45 Å.[85]

The trinuclear species $[Cu_3(dppm)_3\,(\mu_3\text{-OH})](BF_4)_2$ (Figure 16) was found by Harvey and co-workers to be luminescent both at 298 and 77 K.[80] EHMO and density functional calculations resulted in the description of the LUMO as largely copper s and p in character and the HOMO as largely Cu d_{xy} and $d_{x^2-y^2}$ and phosphorus p_x and p_y in character. The emission is assigned to a $^3A_2 \rightarrow {}^1A_1$ transition, i.e., from a luminactive triplet state of {LMCT/(d−s)} character. The polarization ratio of emission was seen to vary gradually from ∼1.0 when excited at 250 nm to ∼0.65 when excited with 340 nm light. This was attributed to splitting of the $^3A_2$ level into E and A_1 spin−orbit sublevels, where the higher energy $E \rightarrow {}^1A_1$ transition is predicted to have a polarization ratio of 1.0 while the $A_1 \rightarrow {}^1A_1$ transition is predicted to be 0.5. The bulky phenyl ligands form a pocket around the Cu(I) centers, which led the authors to examine "host−guest" quenching studies. Stern−Volmer plots were used to quantify luminescence quenching by carboxylate anions such as acetate ($k_q = 1.7 \times 10^8\ M^{-1}\ s^{-1}$) and 4-aminobenzoate ($k_q = 5.1 \times 10^8\ M^{-1}\ s^{-1}$). Given the inability of these carboxylates to quench by energy or electron transfer, the nature of this quenching was assigned to exciplex formation.

Maverick and co-workers[81] have reported a new tetranuclear cluster $[CuN(SiMe_2)_2]_4$ with the anionic amide $N(SiMe_2)_2^-$ bridging the coppers in a square planar Cu_4N_4 motif with adjacent coppers separated by d_{CuCu} values of ∼2.68 Å.[81] The solid has a strong emission band at $\lambda_{max}^{em} = 512$ nm with a lifetime of 30 μs (300 K) and a large Stokes shift. Given that the ligands are saturated, the luminactive state is unlikely to be either ligand-centered $\pi\pi^*$ or MLCT in character. A cluster-centered ES ^{3}CC with mixed {LMCT/(d−s)} character appears likely here as well.

Recently Harvey and co-workers[83] reported new polymeric materials $\{[Cu(dmb)_2Y\}_n$ and $\{[Ag(dmb)_2Y\}_n$ (Y= BF_4^-, NO_3^-, ClO_4^-) composed of Cu(I) and Ag(I) ions linked via the diisocyano ligand 1,8-diisocyano-*p*-menthane (dmb). These materials are weakly luminescent at ambient *T* but exhibit intense luminescence at 77 K (λ_{max}^{em} 517 and 486 nm, respectively). The luminescence decays are multiexponential with lifetimes in the tens of microseconds. With exception of the multiexponential decays (indicating different chromophore environments in the polymer matrix), the behavior parallels the respective monomeric solids $[Cu(CN^tBu)_4]\,BF_4$ ($\lambda_{max}^{em} = 490$ nm, $\tau^{em} = 37$ μs) and $\{Ag(CN^tBu)_4]\,BF_4$ (474 nm, 59 μs) which have been assigned on the basis of EHMO calculations to transitions from MLCT excited states. The similarity of polymer and monomer photophysical properties is unsurprising given the metal−metal distances in the polymers of ∼5 Å.

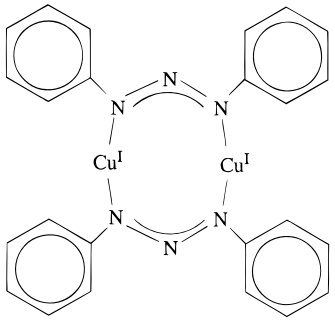

Figure 15. Sketch of $Cu_2(C_6H_5NNNC_6H_5)_2$.

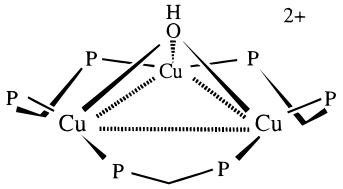

Figure 16. Sketch of $[Cu_3(dppm)_3(\mu^3\text{-OH})]^{2+}$ (dppm = bis-(diphenylphospino)methane.

Metal nuclearity has been used by Zink and co-workers[86] to explain the luminescence properties observed for Cu(I) doped $Na^+-\beta''$-alumina. At very low temperature (∼10 K) two emission bands were seen centered at ∼420 and ∼540 nm. The former was noted to be similar in energy to the emission bands from the $d^9s^1-d^{10}$ transition of the gas-phase free ion Cu^+ (∼450 nm), and this was attributed to monomeric sites in the doped matrix. As *T* was raised to room temperature, this band was quenched, perhaps as a result of the increased mobility of the Cu(I) ions in the alumina, but the green luminescence centered at ∼535 nm remained bright. The latter was attributed to largely immobile Cu(I)−Cu(I) dimers. The lower energies of the dimer emission was explained by invoking metal−metal interactions that led to a decreased band gap between the 3d and 4s orbitals. Extended UV irradiation of the Cu(I)-doped alumina at low temperature led to increases in the green emission at the expense of the blue, and it was concluded that the dimers were formed photochemically, presumably because of the enhanced metal−metal bonding in the excited state resulting from the σ-bonding character of the dimer LUMO. These changes were reversible upon warming the crystal, thus the optical memory represented by the light-induced dimerization can be written, erased, and rewritten.

Similar arguments were presented in later studies by Anpo and co-workers,[87] who noted that when Cu(I) ions were doped into zeolites, the emission depended upon the level of possible aggregation. When Cu(I) ions were included in ZSM-5 and mordenite, which have lower void space/volume and density of ion exchangeable sites, the dominant Cu(I) luminescence observed was blue (~460 nm), characteristic of the emission from a metal-centered excited state of mononuclear Cu(I). The zeolite-Y, with greater void space, showed a strong green emission at ~530 nm attributed to the presence of cuprous ion dimers. These assignments of the nuclearity of Cu(I) species were further supported by XAFS and IR data.

VII. Gold(I) Complexes

Although the present review has focused on the photophysical properties of copper(I) clusters and some structurally analogous silver(I) compounds, it should be noted that there has been considerable interest in the luminactive behavior of mono- and polynuclear gold(I) compounds as well. Some representative studies are listed.[88−95] A detailed discussion of these is outside the scope of the present review; however, certain analogies can be drawn.

Room temperature emissions from gold(I) complexes in solutions and especially as solids with lifetimes in the microsecond range are common as are multiple emissions from polynuclear clusters. In analogy to the copper(I) systems, the luminactive ES have often been assigned as metal-centered (d−s,p) or XMCT states with energies perturbed by Au···Au interactions. Consequently, large Stokes shifts between excitation and emission maxima are also common features. A key feature of the gold(I) chemistry is the greater importance of ground state Au···Au interactions, thus the photophysical properties of even nominally mononuclear Au(I) complexes in the solid state often are affected by this phenomenon.

For example, such interactions were reported by Fackler and co-workers for the complex Au(TPA)Cl (TPA = 1,3,5-triaza-7-phosphaadamantane) and its protonated analogue Au(TPA-HCl)Cl.[88b] The TPA ligand has a small cone angle (102°) which was anticipated to favor intramolecular aurophilic interactions. The closest gold−gold distances in these solids at 193 K were, respectively, 3.092 and 3.322 Å. As 193 K solids, the former displays a broad emission band centered at 676 nm while the latter emits at 596 nm, both of the luminactive ES responsible for both bands being viewed as metal-centered excited states. The lower energy emission for Au(TPA)Cl was attributed to stronger Au···Au interactions leading to destabilization of the HOMO (largely Au $5d_{z^2}$, 6s, and P $3p_z$ in character) and stabilization of the LUMO (principally Au $6p_{x,y}$ and P $3p_{x,y}$). Temperature increases lead to blue shifts of these emission bands, which the authors assigned to thermal expansion. The emission is not seen in solutions of these complexes, an observation attributed to the absence of intermolecular interactions between gold(I) centers. However, it has been noted that such interactions, while common for luminescent Au(I) complexes, are not an absolute requirement, since some strictly mononuclear systems are indeed emissive.[95b]

VIII. Overview and Summary

The above discussion clearly illustrates the point made in the Introduction that the absence of low-lying ligand-field states in copper(I) complexes allows observation of a rich variety of other luminactive excited states. Generally, the emissions are relatively long-lived ($\tau > 1\ \mu$s), strongly suggesting spin forbidden transitions, and quantum yields are often reasonably large even at ambient temperature. The relative stabilities of the two neighboring oxidation states of copper, Cu(0) and Cu(II), allows the direction of charge transfer transitions to depend on the nature of the ligand. As a consequence, emission from ^{3}XLCT, ^{3}LMCT, and ^{3}MLCT luminactive states have been observed with appropriate ligands as well as from ligand-centered $\pi\pi^*$ states and from metal-centered (d−s) states. For polynuclear complexes, a common feature is the mixing of states so that assigning ES with concepts drawn from simple one-electron transitions may be quite misleading. Another critical feature of such clusters is that interactions resulting from short copper−copper distances strongly influence the energies of the luminactive states.

It is these metal−metal interactions and their influence on the nature of the metal-centered and mixed {XLCT/(d−s)} excited states that constitute the most distinguishing photophysical features of the polynuclear copper(I) complexes, relative to their mononuclear analogues. The lowest energy linear combination of Cu 4s orbitals of a Cu_n cluster is metal−metal bonding; thus, the nature of the luminactive ES is strongly dependent on the internuclear distance d_{Cu-Cu}. In this context, a cluster-centered ES of {XMCT/(d−s)} character should be substantially distorted from the ground state structure owing to enhanced metal−metal bonding in the excited state. Such distortions are indicated by the large Stokes shifts experienced by the emission bands as well as the relatively large reorganization energies demonstrated for the electron transfer quenching of certain ^{3}CC states. Since these distortions occur along different nuclear coordinates than do those of XLCT, MLCT, or ligand-centered states, the coupling between the latter and CC ES may be relatively poor, a phenomenon which explains the common occurrence of multiple emissions. In certain cases the various luminactive states may be tunable and moderate perturbations of electronic and structural properties lead to shifts in the relative energetic ordering of the emissive excited states.

Such changes may also be affected by varying experimental conditions such as temperature or hydrostatic pressure; thus, the rigidochromic[30] and thermochromic behavior of polynuclear cuprous compounds offers some promise as environmental sensors or in other novel analytical techniques. For example, Hardt and co-workers some years ago exploited the thermochromic luminescence properties of the CuIL adducts to identify various nitrogen-based ligands by

reaction of their vapors with CuI-saturated papers.[9a] In a similar context, reversible changes in emission spectra resulting from exposing (CuIL) oligomeric solids to vapors of volatile organic compounds (VOCs) offer some interesting possibilities for sensing solvent hydrocarbons.[38] The latter phenomenon is due to structural changes in the crystalline solid mediated by the introduction of solvent vapors. This demonstration of the solid-state lability of such materials emphasizes the importance of coupling structural characterization (e.g., X-ray powder and single-crystal diffraction) with photophysical studies in these systems. Last, ongoing investigations have shown that solid $Cu_4I_4py_4$ (which has a noncentrosymmetric crystal structure) has modest activity in second-harmonic generation, which may be enhanced by using more delocalized ligands with various substituents.[96] Such observations emphasize the exciting potential of these polynuclear compounds for further exploitation of their extraordinarily rich photophysical properties.

IX. Acknowledgments

The preparation of this manuscript and research in these laboratories on the photophysical properties of copper(I) complexes was supported by the National Science Foundation. Dr. Cariati thanks Università di Milano for a postdoctoral fellowship and the Fullbright Commission for support of her postdoctoral stay at UC Santa Barbara.

X. List of Abbreviations

A. Ligands

AdS^-	adamantanethiolate anion
bpym	2,2′-bipyrimidine
$Bz_2{-}18C_6$	dibenzo-18-crown-6
DEN	diethylnicotinamide
dcdpq	6,7-dichloro-2,3-bis(2-pyridyl)quinoxaline
dmb	1,8-diisocyano-*p*-menthane
dmdpq	6,7-dimethyl-2,3-bis(2-pyridyl)quinoxaline
dpbq	2,3-bis(2-pyridyl)benzoquinoxaline
dpmp	2-(diphenylmethyl)pyridine
DPMP	bis(diphenylphosphinomethyl)phenylphosphine
dppm	bis(diphenylphosphino)methane
dppyz	2,3-bis(2-pyridyl)pyrazine
dpq	2,3-bis(2-pyridyl)quinoxaline
dtc	di-*n*-propyl-dithiocarbamate
dtpm	bis[bis(4-methylphenyl)phosphino]methane
en	1,2-diaminoethane or (ethylenediamine)
Et_4en	*N*,*N*′,*N*′-tetraethylethylenediamine
mes	mesityl
morph	morpholine
MT	metallothionein protein
mtc	di-*n*-propyl-monothiocarbamate
pic	methylpyridine
pip	piperidine
pdmp	1-phenyl-3,4-dimethylphospole
PNP	bis(diphenylphosphino)alkyl/arylamine
py	pyridine
quin	quinoline
p-ClAn	*p*-chloroaniline
p-tld	*p*-toluidine

B. Excited-State Labels Used

CC	cluster centered (state)
ES	excited state
GS	ground state
HE	higher energy
LC	ligand centered
LE	lower energy
LF	ligand field
LMCT	ligand to metal charge transfer
MLCT	metal to ligand charge transfer
XLCT	halide (X) to ligand charge transfer
XMCT	halide to metal charge transfer

XI. References

(1) Raston, C. L.; White, A. H. *J. Chem. Soc., Dalton Trans.* **1976**, 2153.
(2) Rath, N. P.; Maxwell, J. L.; Holt, E. M. *J. Chem. Soc., Dalton Trans.* **1986**, 2449.
(3) Dyason, J. C.; Healy, P. C.; Pakawatchai, C.; Patrick, V. A.; White, A. H. *Inorg. Chem.* **1985**, *24*, 1957.
(4) Eitel, E.; Oelkrug, D.; Hiller, W.; Strahle, J. *Z. Naturforsch.* **1980**, *35b*, 1247.
(5) (a) Schmidtke, H. H. In *Physical Methods in Advanced Inorganic Chemistry*; Hill, H. O. A., Day, P., Eds.; Interscience: London, 1968; Chapter 4. (b) Balzani, V.; Carassiti, V. *Photochemistry of Inorganic Compounds*; Academic Press: New York, 1970; Chapter 5. (c) *Concepts in Inorganic Photochemistry*; Adamson, A. W., Fleischauer, P. D., Eds.; Wiley-Interscience: New York, 1975. (d) Crosby, G. A. *J. Chem. Educ.* **1983**, *60*, 791.
(6) (a) Horvath, O. *Coord. Chem. Rev.* **1994**, *135/136*, 303. (b) McMillin, D. R.; McNett, K. M. *Chem. Rev.* **1998**, 1201−1219. (c) Kutal, C. *Coord. Chem. Rev.* **1990**, *99*, 213. (d) Blasse, G. *Adv. Inorg. Chem.* **1990**, *35*, 319.
(7) Kyle, K. R.; Ryu, C. K.; DiBenedetto, J. A.; Ford, P. C. *J. Am. Chem. Soc.* **1991**, *113*, 2954.
(8) (a) Ford, P. C.; Vogler, A. *Acc. Chem. Res.* **1993**, *26*, 220. (b) Ford, P. C. *Coord. Chem. Rev.* **1994**, *132*, 129.
(9) (a) Hardt, H. D.; Pierre, A. *Z. Anorg. Allg. Chem.* **1973**, *402*, 107. (b) Hardt, H. D.; Stoll, H.-J. *Z. Anorg. Allg. Chem.* **1981**, *480*, 193. (c) Hardt, H. D.; Stoll, H.-J. *Z. Anorg. Allg. Chem.* **1981**, *480*, 199.
(10) Dyason, J. C.; Healy, P. C.; Engelhardt, L. M.; Pakawatchai, C.; Patrick, V. A.; Raston, C. L.; White, A. H. *J. Chem. Soc., Dalton Trans.* **1985**, 831.
(11) Ryu, C. K.; Kyle, K. R.; Ford, P. C. *Inorg. Chem.* **1991**, *30*, 3982.
(12) Vogler, A.; Kunkely, H. *J. Am. Chem. Soc.* **1986**, *108*, 7211.
(13) Lindsay, E.; Ford, P. C. *Inorg. Chim. Acta* **1996**, *242*, 51.
(14) (a) Kyle, K. R.; DiBenedetto, J. A.; Ford, P. C. *J. Chem. Soc., Chem. Commun.* **1989**, 714. (b) Kyle, K. R.; Ford, P. C. *J. Am. Chem. Soc.* **1989**, *111*, 5005. (c) Kyle, K. R.; Palke, W. E.; Ford, P. C. *Coord. Chem. Rev.* **1990**, 35.
(15) Rath, N. P.; Holt, E. M. *J. Chem. Soc., Dalton Trans.* **1986**, 2303.
(16) Hardt, H. D.; Pierre, A. *Inorg. Chimica Acta* **1977**, *25*, L59.
(17) Ryu, C. K.; Vitale, M.; Ford, P. C. *Inorg. Chem.* **1993**, *32*, 869.
(18) Lai, D. C.; Zink, J. I. *Inorg. Chem.* **1993**, *32*, 2594.
(19) Hardt, H. D.; Stoll, H.-J. *Z. Anorg.* **1978**, *442*, 221.
(20) Hu, G.; Mains, G. J.; Holt, E. M. *Inorg. Chim. Acta* **1995**, *240*, 559.
(21) Rath, N. P.; Holt, E. M.; Tanimura, K. *Inorg. Chem.* **1985**, *24*, 3934.
(22) de Ahna, H. D.; Hardt, H. D. *Z. Anorg. Allg. Chem.* **1972**, *387*, 61.
(23) Hardt, H. D.; Gechnizdjani, H. *Z. Anorg. Allg. Chem.* **1973**, *397*, 23.
(24) Radjaipour, M.; Oelkrug, D. *Ber. Bunsen-Ges. Phys. Chem.* **1978**, *82*, 159.
(25) Vitale, M.; Palke, W. E.; Ford, P. C. *J. Phys. Chem.* **1992**, *96*, 8329.
(26) Vitalle, M.; Ryu, C. K.; Palke, W. E.; Ford, P. C. *Inorg. Chem.* **1994**, *33*, 561.
(27) Henary, M.; Zink, J. I. *J. Am. Chem. Soc.* **1989**, *111*, 7404.
(28) Engelhardt, L. M.; Healy, P.; Kildea, J. D.; White, A. H. *Aust. J. Chem.* **1989**, *42*, 107.
(29) Wrighton, M.; Morse, D. L. *J. Am. Chem. Soc.* **1974**, *96*, 998.
(30) Tran, D.; Bourassa, J. L.; Ford, P. C. *Inorg. Chem.* **1997**, *36*, 439.
(31) (a) Dossing, A.; Ryu, C. K.; Kudo, S.; Ford, P. C. *J. Am. Chem. Soc.* **1993**, *115*, 5132. (b) Tran, D.; Ryu, C. K.; Ford, P. C. *Inorg. Chem*, **1994**, *33*, 5957.
(32) McClure, L. J.; Ford, P. C. *J. Phys. Chem.* **1992**, *96*, 6640.
(33) Crane, D. R.; Ford, P. C. *J. Am. Chem. Soc.* **1991**, *113*, 8510.
(34) Sutin, N. *Prog. Inorg. Chem.* **1983**, *30*, 441. (b) Marcus, R. A.; Sutin, N. *Biochim. Biophys. Acta* **1985**, *811*, 265.
(35) (a) Casadonte, D. J., Jr.; McMillin, D. R. *J. Am. Chem. Soc.* **1987**, *109*, 9. (b) Gamache, R. E., Jr.; Rader, R. A.; McMillin, D. R. *J. Am. Chem. Soc.* **1985**, *107*, 1141.

(36) Maini, L.; Bourassa, J.; Ford, P. C. Unpublished work described in the Tesi di Laurea di L. Maini, Universitá di Bologna, 1996.
(37) Li, D.; Yip, H.-K.; Che, C.-M.; Zhou, Z.-Y.; Mak, T. C. W.; Liu, S.-T. *J. Chem. Soc., Dalton Trans.* **1992**, 2445.
(38) Cariati, E.; Bourassa, J. L.; Ford, P. C. *Chem. Commun.* **1998**, 1623.
(39) Henary, M.; Wootton, J. L.; Khan, S. I.; Zink, J. I. *Inorg. Chem.* **1997**, *36*, 796.
(40) Simon, J. A.; Palke, W. E.; Ford, P. C. *Inorg. Chem.* **1996**, *35*, 6413.
(41) Vitale, M. Ph.D. Dissertation, University of California, Santa Barbara, 1993.
(42) Engelhardt, L. M.; Papasergio, R. I.; White, A. H. *Aust. J. Chem.* **1984**, *37*, 2207−13.
(43) Sabin, F.; Ryu, C. K.; Ford, P. C.; Vogler, A. *Inorg. Chem.* **1992**, *31*, 1941.
(44) Bourassa, J. L. Ph.D. Dissertation, University of California, Santa Barbara, 1998.
(45) Fujisawa, K.; Imai, S.; Kitajima, N.; Moro-oka, Y. *Inorg. Chem.* **1998**, *337*, 168.
(46) Baumgartner, M.; Schmalle, H.; Dubler, E. *Polyhedron* **1990**, *9*, 1155.
(47) (a) Yam, V. W. W.; Lee, W. K.; Lai, T. F. *J. Chem. Soc., Chem. Commun.* **1993**, 1571. (b) Yam, V. W.−W.; Lo, K. K.−W.; Cheung, K.-K. *Inorg. Chem.* **1996**, *35*, 3459. (c) Yam, V. W. W.; Lo, K. K. W.; Wang, C. R.; Cheung, K. K. *Inorg. Chem.* **1996**, *35*, 5116. (d)Yam, V. W.−W.; Lo, K. K.−W.; Wang, C.-R.; Cheung, K.-K. *J. Phys. Chem. A* **1997**, *101*, 4666. (e) Yam, V. W.−W.; Lo, K. K.−W. *Comments Inorg. Chem.* **1997**, *19*, 209. (e) Wang, C. R.; Lo, K. K.-W.; Fung, W. K.-M.; Yam, V. W.-W. *Chem. Phys. Lett.* **1998**, *296*, 505.
(48) Rasmussen, J. C.; Toftlund, H.; Nivorzhkin, A. N.; Bourassa, J.; Ford, P. C. *Inorg. Chim. Acta* **1996**, *251*, 221.
(49) (a) Knotter, D. M.; Blasse, G.; van Vliet, J. P. M.; van Koten, G. *Inorg. Chem.* **1992**, *31*, 2196−2201. (b) Knotter, D. M.; van Koten, G.; van Maanen, H.; Grove, D. M.; Spek, A. L. *Angew. Chem., Int. Ed. Engl.* **1989**, *28*, 341.
(50) (a) Fujisawa, K.; Imai, S.; Kitajima, N.; Moro-oka, Y. *Inorg. Chem.* **1998**, *337*, 168. (b) Chan, C.-K.; Guo, C.-X.; Wang, R.-J.; Mak, T. C. W.; Che, C.-M. *J. Chem. Soc., Dalton Trans.* **1995**, 753.
(51) (a) The ionization energies of atomic Cu and Ag are 6.232×10^4 and 6.111×10^4 cm^{-1}, respectively.[51b] (b) *CRC Handbook of Chemistry and Physics*, 71st ed.; Lide, D. R., Ed.; CRC Press: Boston, 1990; pp 10−210.
(52) Jørgensen, C. K. Inorganic Complexes; Academic Press: London, 1963; p 136.
(53) Lever, A. B. P. *Inorganic Electronic Spectroscopy*, 2nd ed.; Elsevier: Amsterdam, 1984; p 221.
(54) Kita, H.; Migake, S.; Tanaka, K.; Tanaka, T. *Bull Chem. Soc., Jpn.* **1979,** *52*, 3532.
(55) Moore, C. E. *Natl. Stand. Ref. Data Ser. (U.S. Natl. Bur. Stand.)* **1971**, *NSRDS−NBS 35* 51, 116.
(56) (a) Jennische, P.; Hesse, R. *Acta Chem. Scand.* **1971**, *25*, 423. (b) Hesse, R.; Arva, U. *Acta Chem. Scand.* **1970**, *24*, 1355.
(57) Dance, I. G. *Polyhedron* **1986**, *5*, 1037−1104.
(58) (a) Stillman, M. J.; Zelazowski, A. J.; Szymanska, J.; Gasnya, Z. *Inorg. Chim. Acta* **1989**, *161*, 275. (b) *Metallothioneins*; Stillman, M. J., Shaw, C. F., III, Suzuki, K. T., Eds.; VCH Publishers: New York, 1992. (c) Stillman, M. J. *Coord Chem. Rev.* **1995**, *144*, 461.
(59) Green, A. R.; Stillman, M. J. *Inorg. Chim. Acta* **1994**, *226*, 275.
(60) Li, Y.-J.; Weser, U. *Inorg. Chem.* **1992**, *31*, 5526.
(61) (a) Green, A. R.; Presta, A.; Gasyna, Z.; Stillman, M. J. *Inorg. Chem.* **1994**, *33*, 4159. (b) Green, A. R.; Stillman, M. J. *Inorg. Chem.* **1996**, *35*, 2799.
(62) Yam, V. W.−W.; Lee, W.-K.; Cheung, K. K.; Lee, H.-K.; Leung, W.-P. *J. Chem. Soc., Dalton Trans.* **1996**, 2889.
(63) Yam, V. W.−W.; Fung, W. K.−M.; Wong, M.-T. *Organometallics* **1997**, *16*, 1772.
(64) Yam, V. W.−W.; Lee, W.-K.; Cheung, K.-K.; Crystall, B.; Phillips, D. *J. Chem. Soc., Dalton Trans.* **1996**, 3283.
(65) Yam, V. W.−W.; Lee, W.-K.; Lai, T.-F. *Organometallics* **1993**, *12*, 2383.
(66) Yam, V. W.−W.; Fung, W. K.−M.; Cheung, K.-K. *Chem. Commun.* **1997**, 963.
(67) Yam, V. W.−W.; Fung, W. K.−M.; Cheung, K.-K. *Angew. Chem., Int. Ed. Engl.* **1996**, *35*, 1100.
(68) Yam, V. W.−W.; Choi, S. W.−K.; Chan, C.-L.; Cheung, K.-K. *Chem. Commun.* **1996**, 2067.
(69) Yam, V. W.−W.; Lee, W.-K.; Cheung, K.-K. *J. Chem. Soc., Dalton Trans.* **1996**, 2335.
(70) (a) Yam, V. W.-W.; *J. Photochem. Photobiol. A: Chem.* **1997**, *106*, 75. (b) Yam, V. W.-W.; Lo, K. K.; Fung, W. K.-M.; Wang, C. R. *Coord. Chem. Rev.* **1998**, *171*, 17.
(71) Yam, V. W.-W.; Lee, W.-K.; Yeung, P. K. Y.; Phillips, D. *J. Phys. Chem.* **1994**, *98*, 7545.
(72) Yam, V. W.-W.; Fung, W. K.-M.; Cheung, K. K. *Organometallics* **1998**, *17*, 3293.
(73) Yam, V. W.-W.; Fung, W. K.-M.; Cheung, K.-K. *Organometallics* **1997**, *16*, 2032.
(74) Vogler, C.; Hausen, H.-D.; Kaim, W.; Kohlman, S.; Kramer, H. E. A.; Rieker, J. *Angew. Chem., Int. Ed. Engl.* **1989**, *28*, 1659.
(75) Yam, V. W.−W.; Lo, K. K.−W. *J. Chem. Soc., Dalton Trans.* **1995**, 499.
(76) Harvey, P. D. *Inorg. Chem.* **1995**, *34*, 2019.
(77) Field, J. S.; Haines, R. J.; Warwick, B. *Polyhedron* **1996**, *15*, 3741.
(78) (a) Li, D.; Che, C.-M.; Kwong, H.-L.; Yam, V. W.−W. *J. Chem. Soc., Dalton Trans.* **1992**, 3325. (b) Li, D.; Che, C.-M.; Wong, W.-T.; Shieh, S.-J.; Peng, S.-M. *J. Chem. Soc., Dalton Trans.* **1993**, 653.
(79) Harvey, P. D.; Drouin, M.; Zhang, T. *Inorg. Chem.* **1997**, *36*, 4998.
(80) Provencher, R.; Harvey, P. D. *Inorg. Chem.* **1996**, *35*, 2235.
(81) James, A. M.; Laxman, R. K.; Fronczek, F. R.; Maverick, A. W. *Inorg. Chem.* **1998**, *37*, 3785.
(82) Chan, C.-K.; Cheung, K.-K.; Che, C.-M. *Chem. Commun.* **1996**, 227.
(83) (a) Fortin, D.; Drouin, M.; Turcotte, M.; Harvey, P. D. *J. Am. Chem. Soc.* **1997**, *119*, 531. (b) Fortin, D.; Drouin, M.; Harvey, P. D. *J. Am. Chem. Soc.* **1998**, *120*, 5357.
(84) Ford, P. C.; Rudd, DeF. P.; Gaunder, R.; Taube, H. *J. Am. Chem. Soc.* **1968**, *90*, 1187.
(85) Brown, J. D.; Dunitz, J. D. *Acta Crystallogr.* **1961**, *14*, 480.
(86) Barrie, J. D.; Dunn, B.; Hollingsworth, G.; Zink, J. I. *J. Phys. Chem.* **1989**, *93*, 3958.
(87) Yamashita, H.; Matsuoka, M.; Tsuji, K.; Shioya, Y.; Anpo, M.; Che, M. *J. Phys. Chem.* **1996**, *100*, 397.
(88) (a) Assefa, Z.; McBurnett, B. G.; Staples, R. J.; Fackler, J. P., Jr.; Assmann, B.; Angermaier, K.; Schmidbaur, H. *Inorg. Chem.* **1995**, *34*, 75. (b) Forward, J. M.; Bohmann, D.; Fackler, J. P., Jr.; Staples, R. J. *Inorg. Chem.* **1995**, *34*, 6330. (c) Forward, J. M.; Assefa, Z.; Fackler, J. P., Jr. *J. Am. Chem. Soc.* **1995**, *117*, 9103.
(89) Hanna, S. D.; Khan, S. I.; Zink, J. I. *Inorg. Chem.* **1996**, *35*, 5813−5819. Hanna, S. D.; Zink, J. I. *Inorg. Chem.* **1996**, *35*, 297.
(90) Mansour, M. A.; Connick, W. B.; Lachicotte, R. J.; Gysling, H. J.; Eisenberg, R. *J. Am. Chem. Soc.* **1998**, *120*, 1329.
(91) (a) Fung, E. Y.; Olmstead, M. M.; Vickery, J. C.; Balch, A. L. *Coord. Chem. Rev.* **1998**, *171*, 151−159. (b) Vickery, J. C.; Olmstead, M. M.; Fung, E. Y.; Balch, A. L. *Angew. Chem., Int. Ed. Engl.* **1997**, *36*, 1179.
(92) (a) Strasser, J.; Yersin, H.; Patterson, H. H. *Chem. Phys. Lett.* **1998**, *295*, 95−98. (b) Omary, M. A.; Patterson, H. H. *J. Am. Chem Soc.* **1998**, *120*, 7696−7705.
(93) (a) Chan, W. H.; Mak, T. C. W.; Che, C. M. *J. Chem. Soc., Dalton Trans.* **1998**, 2275−2276. (b) Xiao, H.; Weng, Y. X.; Wong, W. T.; Mak, T. C. W.; Che, C. M. *J. Chem. Soc., Dalton Trans.* **1997**, 221−226.
(94) (a) Yam, V. W. W.; Cheng, E. C. C.; Cheung, K. K. *Angew. Chem., Int. Ed. Engl.* **1999**, *38*, 197−199. (b) Yam, V. W. W.; Lee, W. K. *J. Chem. Soc., Dalton Trans.* **1993**, 2097−2100.
(95) (a) Irwin, M. J.; Vittal, J. J.; Puddephatt, R. J. *Organometallics* **1997**, *16*, 3541. (b) Jones, W. B.; Yuan, J.; Narayanaswam, R.; Young, M. A.; Elder, R. C.; Bruce, A. E.; Bruce, M. R. M. *Inorg. Chem.* **1995**, *34*, 1996. (c) McCleskey, T. M.; Gray, H. B. *Inorg. Chem.* **1992**, *31*, 1734.
(96) Cariati, E.; Ryu, C. K.; Ford, P. C. Unpublished work in progress.

CR960109I